Int. J. Solids Structures, 1970, Vol. 6, pp. 829 to 857. Pergamon Press. Printed in Great Britain

TWISTING AND EXPANSION OF A HOLE IN A NON-UNIFORM DISK†

JENN-MING CHERN‡ and S. NEMAT-NASSER§

Department of the Aerospace and Mechanical Engineering Sciences,
University of California, San Diego, La Jolla, California

Abstract—Finite and infinitesimal deformation of an infinitely extended, axisymmetric disk of a non-uniform initial thickness with a circular hole is considered. The disk is loaded along the interior surface of the hole by pressure and twisting moment of non-decreasing magnitudes. A state of plane stress is assumed and the incremental theory of plasticity is used. The material of the disk is assumed to be rigid–plastic for finite deformation and elastic–plastic for infinitesimal deformation. The analyses are based on the Tresca yield criterion and the isotropic hardening law, and emphasis is placed on the effects of the twisting moment, hardening parameter and loading path on the solution. Detailed results and comparisons are given for an initially uniform and an initially conical disk. Finally, comparison is made between solutions for elastic–plastic and rigid–plastic disks, revealing that the stress field is only slightly affected by the elastic strains.

NOTATION

A	a function of t
AB, B, etc.	plastic regimes in initial yielding
$A'B'$, B', etc.	plastic regimes in subsequent yielding
D	a function of m, n and ρ_1
E	Young's modulus
$\bar{E}$	$= E/\sigma_0$
G	a function of n, R_0 and ρ_0
$G_1, G_2, \mathscr{H}$	functions of $\bar{\sigma}$, R and $\bar{\rho}_0$
H_0, H	$H_0 = h_0/\alpha_0$, $H = h/\alpha_0$
P, m	dimensionless load parameters defining pressure and twisting moment, respectively
R_0, R	$R_0 = r_0/b_0$, $R = r/b_0$
U_r, U_θ	dimensionless radial and circumferential displacement-components; $U_r = u_r/b_0$, $U_\theta = u_\theta/b_0$
V_r, V_θ	dimensionless radial and circumferential velocity-components; $V_r = v_r/b_0$, $V_\theta = v_\theta/b_0$
$W_p\sigma_0$	plastic work/unit volume
a	hardening parameter
b_0, b	radius of circular hole in undeformed and deformed states, respectively
$\bar{b}$	$= b/b_0$
e	a function of t
f	yield function
h_0, h	thickness of the disk in undeformed and deformed states, respectively; $h_0 = \alpha_0(r_0/b_0)^n$
r_0, r	radial distance in undeformed and deformed states, respectively
t	time parameter
u_r, u_θ	radial and circumferential displacement-components
v_r, v_θ	radial and circumferential velocity-components
Φ_1, Φ_2	functions of R and $\bar{\rho}_0$

† The results of this paper were obtained in the course of research sponsored under Contract No. N00014-67-A-0109-0003, Task NR 064-496 by the Office of Naval Research, Washington, D.C.

‡ Postgraduate Research Engineer; presently in: Division of Engineering, Brown University, Providence, Rhode Island.

§ Associate Professor of Applied Mechanics.

Γ_1, Γ_2	curves in the plane of load parameters
α_0, n	constants defining the initial thickness of disk; $h_0 = \alpha_0(r_0/b_0)^n$
α_0, α	thickness of the disk at the edge of the hole in undeformed and deformed states, respectively
β	constant depending on n and ν
η	material constant; $\eta = a\sigma_0/E$
$\varepsilon_r', \varepsilon_\theta', \varepsilon_{r\theta}', \varepsilon_z'$	elastic strains
$\varepsilon_r'', \varepsilon_\theta'', \varepsilon_{r\theta}'', \varepsilon_z''$	plastic strains
ρ_0	interface between rigid and neutral plastic regions
$\bar{\rho}_0$	interface between elastic and elastic–plastic regions
ρ_1	interface between neutral and active plastic regions
ρ_2	interface between active plastic regions
μ	$= \dot{P}/\dot{m}, \dot{m} \neq 0$
λ	a nonnegative function depending on state of stress
ν	Poisson's ratio
ψ	a function of $\bar{\sigma}$ and R
σ_0, σ	initial and subsequent yield stresses in simple tension
$\bar{\sigma}$	$= \sigma/\sigma_0$
$\sigma_r, \sigma_\theta, \sigma_{r\theta}$	stress components
$\bar{\sigma}_r, \bar{\sigma}_\theta, \bar{\sigma}_{r\theta}$	$\bar{\sigma}_r = \sigma_r/\sigma_0, \bar{\sigma}_\theta = \sigma_\theta/\sigma_0, \bar{\sigma}_{r\theta} = \sigma_{r\theta}/\sigma_0$
θ_0, θ	angular coordinates of particles in undeformed and deformed states, respectively
$(\ldots)^{\cdot}$	material-time-derivative of $(\ldots)$

1. INTRODUCTION

THE problem of the expansion of a circular hole in an infinitely extended disk of a uniform initial thickness, subject to a pressure applied along the edge of the hole, has been considered by Taylor [1], Hill [2], Prager [3] and Hodge and Sankaranarayanan [4]. A similar problem, but for an initially non-uniform disk, and under the assumption of plane stress, has been considered by Alexander and Ford [5], Rogers [6], Nemat-Nasser [7], Chern and Nemat-Nasser [8] and Chern [9]. In the case when a pressure is applied on the interior surface of the hole, a similarity solution becomes possible and the problem may be characterized by only one time–space independent variable.

For a combined loading problem, where the interior surface of the hole is subjected to both a pressure and a shear loading, the geometric similarity does not exist, and the solution becomes more complicated. Nordgren and Naghdi [10] considered the problem of simultaneous expansion and twisting of the interior surface of a hole in a finite or infinite plastic plate of a uniform initial thickness, using the yield conditions of Tresca and Mises and the associate flow rules together with an isotropic hardening law. A complete solution is given by these authors for Tresca's yield criterion and its flow rule. These authors [11] also analyzed a similar problem using an infinitesimal theory, and discussed the unloading solution.

In this paper, we first consider the axisymmetric, finite expansion and twisting of a circular hole in a disk of a variable initial thickness. A state of plane stress is assumed, and Tresca's yield criterion together with the isotropic hardening law is used. Detailed numerical results are given for the initially uniform and conical disks, and the effects of twisting moment, hardening parameter, and loading path on the field quantities are investigated. The problem is then reconsidered on the basis of an infinitesimal theory, including the elastic strains. The effect of the elastic strains on the field quantities, and the possible justifications for the assumption of rigid–plasticity are examined. We note that, from the solutions presented in this paper, some of the results of the previous investigations [10, 11] are deduced as special cases.

2. STATEMENT OF PROBLEM AND BASIC EQUATIONS

We consider the axisymmetric expansion and twisting of a circular hole in an infinitely extended, axisymmetric disk of the initial contour $h_0 = \alpha_0(r_0/b_0)^n$, where r_0 measures radial distance in the undeformed state, b_0 is the initial radius of the hole, and α_0 and n are constants; α_0 is the initial thickness of the disk at the edge of the hole. Let the radius and the thickness at the edge of the hole in the deformed state be denoted by b and α, respectively. On the inner boundary $r = b$, the disk is subjected to a normal compressive force of magnitude $P\alpha_0\sigma_0$, per unit circumferential length, and a twisting moment of total magnitude $m\pi\alpha_0 b_0^2\sigma_0$, where σ_0 is the initial yield stress in simple tension for the considered material, and P and m are the dimensionless load parameters which are assumed to be non-decreasing functions of a time parameter t. Since a quasi-static loading is considered, t denotes a conveniently selected, monotonically increasing (or perhaps decreasing) parameter.

Referring to cylindrical coordinates (r, θ, z), we denote the Eulerian stress-components by σ_r, σ_θ, $\sigma_{r\theta}$ and σ_z, the displacement-components by u_r and u_θ, the velocity-components by v_r and v_θ, the current thickness of the disk by h, the Young's modulus by E, and introduce the following dimensionless quantities:

$$\begin{aligned} \{\bar{\sigma}_r, \bar{\sigma}_\theta, \bar{\sigma}_{r\theta}, \bar{\sigma}_z, \bar{E}\} &= \{\sigma_r, \sigma_\theta, \sigma_{r\theta}, \sigma_z, E\}/\sigma_0 \\ \{H, H_0, \bar{\alpha}, \bar{b}\} &= \{h, h_0, \alpha, b\}/\alpha_0, \\ \{R, R_0, U_r, U_\theta, V_r, V_\theta\} &= \{r, r_0, u_r, u_\theta, v_r, v_\theta\}/b_0. \end{aligned} \tag{2.1}$$

For a state of plane stress with $\bar{\sigma}_z = 0$, the non-zero stress-components satisfy the following equations of equilibrium:

$$\frac{\partial}{\partial R}(H\bar{\sigma}_r) + \frac{H}{R}(\bar{\sigma}_r - \bar{\sigma}_\theta) = 0, \tag{2.2a}$$

$$\frac{\partial}{\partial R}(HR^2\bar{\sigma}_{r\theta}) = 0, \tag{2.2b}$$

and the velocity-components are given by

$$V_r = \dot{R}(R, t), \qquad V_\theta = R\dot{\theta}(R, t), \tag{2.3}$$

where a superposed dot stands for the material-time-derivative, that is, partial time-derivative with the initial particle position, R_0, held fixed. Hence, the non-zero components of the strain-rate tensor are

$$\begin{aligned} \dot{\varepsilon}_r &= \frac{\partial V_r}{\partial R}, \qquad \dot{\varepsilon}_\theta = \frac{V_r}{R} \\ \dot{\varepsilon}_{r\theta} &= \frac{1}{2}R\frac{\partial}{\partial R}\left(\frac{V_\theta}{R}\right), \qquad \dot{\varepsilon}_z = \frac{\dot{H}}{H}, \end{aligned} \tag{2.4}$$

where $\dot{\varepsilon}_r$ and $\dot{\varepsilon}_\theta$ satisfy the following compatibility condition:

$$\dot{\varepsilon}_r = \frac{\partial}{\partial R}(R\dot{\varepsilon}_\theta). \tag{2.5}$$

We note that in the infinitesimal theory, no distinction needs to be made between R and R_0, and, thus, (2.4) may be written as

$$\varepsilon_r = \frac{\partial U_r}{\partial R}, \qquad \varepsilon_\theta = \frac{U_r}{R}, \qquad 2\varepsilon_{r\theta} = \frac{\partial U_\theta}{\partial R} - \frac{U_\theta}{R}, \qquad H = H_0(1+\varepsilon_z). \tag{2.6}$$

For an elastic–plastic material, the strain-rate tensor may be decomposed into the elastic and plastic parts which will be designated by the superposed prime and double primes, respectively. The elastic strain-rates are related to the stress-rates by Hooke's law

$$\{\dot{\varepsilon}'_r, \dot{\varepsilon}'_\theta, \dot{\varepsilon}'_{r\theta}, \dot{\varepsilon}'_z\} = \{\dot{\bar{\sigma}}_r - \nu\dot{\bar{\sigma}}_\theta, \dot{\bar{\sigma}}_\theta - \nu\dot{\bar{\sigma}}_r, (1+\nu)\dot{\bar{\sigma}}_{r\theta}, -\nu(\dot{\bar{\sigma}}_r + \dot{\bar{\sigma}}_\theta)\}/\bar{E}, \tag{2.7}$$

where ν is Poisson's ratio. The plastic strain-rates are related to the stress-rates by the plastic flow rules.

For the state of plane stress with $\bar{\sigma}_z = 0$, the dimensionless principal stresses $\bar{\sigma}_1$ and $\bar{\sigma}_2$ are given by

$$\{\bar{\sigma}_1, \bar{\sigma}_2\} = \tfrac{1}{2}(\bar{\sigma}_r + \bar{\sigma}_\theta) \mp [\tfrac{1}{4}(\bar{\sigma}_r - \bar{\sigma}_\theta)^2 + \bar{\sigma}_{r\theta}^2]^{\frac{1}{2}}. \tag{2.8}$$

According to Tresca's yield criterion and isotropic hardening law, with yield stress in simple tension denoted by $\sigma \equiv \bar{\sigma}\sigma_0$, and the hardening parameter designated by a, the yield function has the form

$$f \equiv \max\{|\bar{\sigma}_1|, |\bar{\sigma}_2|, |\bar{\sigma}_1 - \bar{\sigma}_2|\} - \bar{\sigma} = 0, \tag{2.9}$$

where

$$\dot{\bar{\sigma}} = a\dot{W}_p \quad \text{with} \quad \bar{\sigma} = 1 \quad \text{for} \quad W_p = 0, \tag{2.10a}$$

and

$$W_p = \int_0^t (\bar{\sigma}_r\dot{\varepsilon}''_r + \bar{\sigma}_\theta\dot{\varepsilon}''_\theta + 2\bar{\sigma}_{r\theta}\dot{\varepsilon}''_{r\theta})\,\mathrm{d}t, \tag{2.10b}$$

where $W_p\sigma_0$ is the work expended/unit volume in plastic deformation. Tresca's yield function (2.9) defines a yield hexagon in the $\bar{\sigma}_1$, $\bar{\sigma}_2$-plane (Fig. 1). In accordance with the isotropic hardening law, the initial yield hexagon (with $\bar{\sigma} = 1$) expands uniformly as the plastic deformation continues. As we shall see, only the plastic regimes defined by the side AB and the corner B of the yield hexagon in Fig. 1 are of interest to us. On the regular regime AB, the yield function becomes

$$f_{AB} \equiv (\bar{\sigma}_r - \bar{\sigma}_\theta)^2 + 4\bar{\sigma}_{r\theta}^2 - \bar{\sigma}^2 = 0, \tag{2.11a}$$

and the corresponding plastic strain-rates, as determined by the flow rules, are

$$\{\dot{\varepsilon}''_r, \dot{\varepsilon}''_\theta, \dot{\varepsilon}''_{r\theta}, \dot{\varepsilon}''_z\} = \frac{\dot{\lambda}}{2}\{\bar{\sigma}_r - \bar{\sigma}_\theta, \bar{\sigma}_\theta - \bar{\sigma}_r, 2\bar{\sigma}_{r\theta}, 0\}. \tag{2.11b}$$

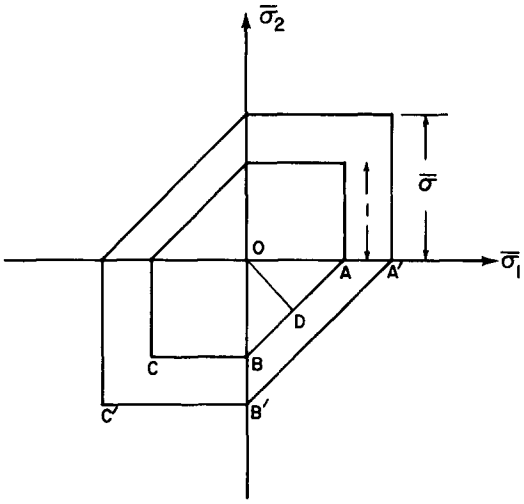

FIG. 1. Tresca's yield function and isotropic hardening law.

At the singular regime B, on the other hand, we have

$$\bar{\sigma}_r\bar{\sigma}_\theta = \bar{\sigma}_{r\theta}^2, \qquad \bar{\sigma}_r+\bar{\sigma}_\theta = -\bar{\sigma}, \tag{2.12a}$$

$$\{\dot{\bar{\varepsilon}}_r'', \dot{\bar{\varepsilon}}_\theta'', \dot{\bar{\varepsilon}}_{r\theta}'', \dot{\bar{\varepsilon}}_z''\} = \frac{\dot{\lambda}}{2}\{\bar{\sigma}_r-\gamma\bar{\sigma}_\theta, \bar{\sigma}_\theta-\gamma\bar{\sigma}_r, (1+\gamma)\bar{\sigma}_{r\theta}, (1-\gamma)\bar{\sigma}\}. \tag{2.12b}$$

In (2.11) and (2.12)

$$\dot{\lambda} \geq 0, \qquad 0 \leq \gamma \leq 1, \tag{2.13}$$

and the plastic incompressibility

$$\dot{\bar{\varepsilon}}_r'' + \dot{\bar{\varepsilon}}_\theta'' + \dot{\bar{\varepsilon}}_z'' = 0 \tag{2.14}$$

is also used. We note that a state is on the regular regime AB (or $A'B'$, see Fig. 1) if $\bar{\sigma}_2 < 0 < \bar{\sigma}_1$, which is fulfilled provided that

$$\bar{\sigma}_r\bar{\sigma}_\theta < \bar{\sigma}_{r\theta}^2, \tag{2.15}$$

as can be seen from (2.8). Substitution of (2.11) and (2.12) into (2.10) shows that, on the regimes AB and B, the isotropic hardening law takes on the form

$$\dot{\bar{\sigma}} = \tfrac{1}{2}\dot{\lambda}a\bar{\sigma}^2. \tag{2.16}$$

For the loadings considered here, the stress field must satisfy the boundary conditions

$$\bar{\sigma}_r = -P(t)/\bar{\alpha} \quad \text{at} \quad R = \bar{b}, \tag{2.17a}$$

$$\bar{\sigma}_{r\theta} = \tfrac{1}{2}m(t)/\bar{\alpha}\bar{b}^2 \quad \text{at} \quad R = \bar{b}, \tag{2.17b}$$

and for points at infinity we must have

$$\lim_{R\to\infty}\{\bar{\sigma}_r, \bar{\sigma}_\theta, \bar{\sigma}_{r\theta}, U_r, U_\theta\} = 0. \tag{2.17c}$$

The solution of (2.2b) with the boundary condition (2.17b) is

$$\bar{\sigma}_{r\theta} = \tfrac{1}{2}m(t)/HR^2. \tag{2.18}$$

When no plastic deformation has taken place, the disk is fully elastic, $\varepsilon_r = \varepsilon_r'$, $\varepsilon_\theta = \varepsilon_\theta'$ and $\varepsilon_{r\theta} = \varepsilon_{r\theta}'$. In this case, the infinitesimal theory may be used, and hence we set $R = R_0$ in the equations of equilibrium. Upon substitution of the expression for the initial contour of the disk into the equation of radial equilibrium (2.2a), we obtain

$$\bar{\sigma}_\theta = (n+1)\bar{\sigma}_r + R\frac{\partial\bar{\sigma}_r}{\partial R}. \tag{2.19}$$

We may eliminate $\bar{\sigma}_\theta$ from (2.19) by using stress–strain relations [i.e. (2.7) without superposed dots] and the compatibility condition [i.e. (2.5) without superposed dots], and solve the resulting second order ordinary differential equation for $\bar{\sigma}_r$, subject to the boundary condition (2.17c), obtaining

$$\bar{\sigma}_r = -AR^{-\beta}. \tag{2.20a}$$

From (2.19), $\bar{\sigma}_\theta$ now is

$$\bar{\sigma}_\theta = A(\beta-n-1)R^{-\beta}, \tag{2.20b}$$

where A is a function of t, and

$$\beta = \tfrac{1}{2}[n+2+(n^2-4nv+4)^{\frac{1}{2}}]. \tag{2.20c}$$

The strain can then be readily obtained by substitution from (2.20) and (2.18) into the stress–strain relations, yielding

$$\varepsilon_r = -\frac{A}{\bar{E}}[1+v(\beta-n-1)]R^{-\beta}, \tag{2.21a}$$

$$\varepsilon_\theta = \frac{A}{\bar{E}}[(\beta-n-1)+v]R^{-\beta}, \tag{2.21b}$$

$$\varepsilon_{r\theta} = \frac{1+v}{2\bar{E}}mR^{n+2}, \tag{2.21c}$$

$$\varepsilon_z = \frac{Av}{\bar{E}}(n+2-\beta)R^{-\beta}. \tag{2.21d}$$

Substituting (2.21) into (2.6), integrating the resulting equations with respect to R from R to ∞, and using the boundary condition (2.17c), we obtain

$$U_r = \frac{A}{\bar{E}}[(\beta-n-1)+v]R^{\beta-1}, \tag{2.22a}$$

$$U_\theta = -\frac{m}{\bar{E}}\frac{1+v}{n+2}R^{n+1}, \tag{2.22b}$$

$$H = H_0\left[1+\frac{Av}{\bar{E}}(2+n-\beta)R^\beta\right]. \tag{2.22c}$$

We note that for $n = 0$, (2.22c) reduces to $H = H_0$. Since the disk is fully elastic, the integration constant A (as a function of t) is determined from (2.20a) and the boundary condition (2.17a) (with $\bar{\alpha} = 1$) as

$$A = P(t). \tag{2.23}$$

For the Tresca yield condition considered here, the plastic deformation initiates at $R = 1$ with the vanishing of the initial yield function, given by (2.11a), which corresponds to the regime AB. Substitution from (2.18) and (2.20) into (2.11a) now results in

$$(\beta - n)^2 P^2 + m^2 \leq 1 \tag{2.24}$$

which assures that the disk is fully elastic and which defines a domain bounded by the ellipse Γ_1, whose equation is $(\beta - n)^2 P^2 + m^2 = 1$, and the P-, m-axes in the plane of the load parameters m and P (see Fig. 2).

For further loading in violation of (2.24), plastic deformations take place at the vicinity of the hole.

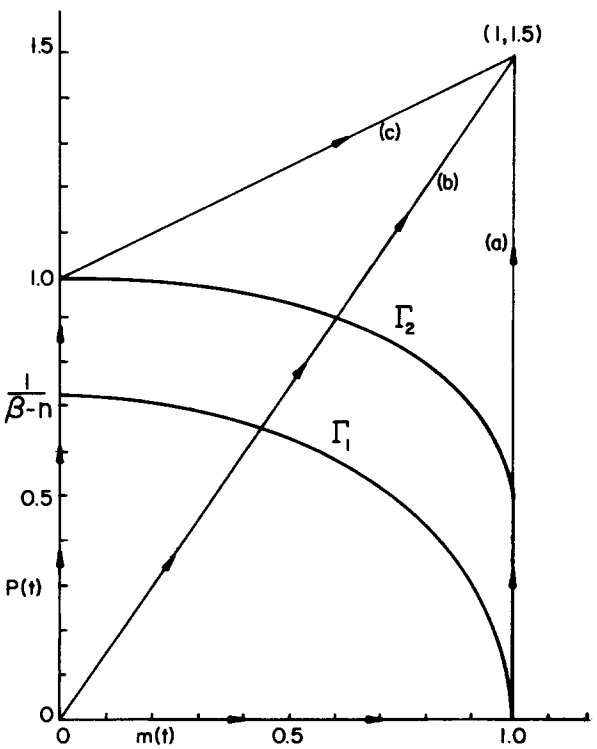

FIG. 2. Plane of load parameters m and P.

3. FINITE DEFORMATION OF A RIGID–PLASTIC DISK

For rigid–plastic disk and upon further loading that violates (2.24), a plastic region corresponding to the regime AB (Fig. 1) develops in the part of the disk defined by $1 \leq R \leq \rho_0$, where ρ_0, as a function of t, is the dimensionless radius of the plastic–rigid interface. In the rigid region $R = R_0 \geq \rho_0$, the stress and the displacement fields are obtained from the corresponding elastic solution by setting $\nu = \frac{1}{2}$ and $\bar{E} = \infty$. Therefore, (2.21) and (2.22) show that

$$V_r = V_\theta = U_r = U_\theta = \varepsilon_r = \varepsilon_\theta = \varepsilon_{r\theta} = \varepsilon_z = H - H_0 = 0, \qquad R \geq \rho_0. \tag{3.1}$$

The stress-state is still given by (2.18) and (2.20) with

$$A = (\beta - n)^{-1} \rho_0^{\beta} (1 - m^2 \rho_0^{-2n-4})^{\frac{1}{2}} \tag{3.2}$$

which is obtained from the condition (2.11a) at $R = \rho_0$ with $\bar{\sigma} = 1$, and β is given by (2.20c) with $\nu = \frac{1}{2}$. Since $\beta > n$, A in (3.2) is always positive, rendering $\bar{\sigma}_r < 0 < \bar{\sigma}_\theta$ for $n < 2$ and $R > \rho_0$. Moreover, from the continuity of $\bar{\sigma}_r$, $\bar{\sigma}_{r\theta}$, and f_{AB} at $R = \rho_0$, it follows that $\bar{\sigma}_\theta$ is also continuous there. Equations (2.4) and (2.11b) now yield

$$RV_r = \dot{e}(t) \tag{3.3}$$

in the regime AB, where $\dot{e}(t)$ is independent of R. Since V_r is continuous at $R = \rho_0$ and vanishes for $R = \rho_0^+$, we conclude that $V_r = 0$ everywhere. Thus, using (2.3) and (2.4), we arrive at

$$\dot{\varepsilon}_r = \dot{\varepsilon}_\theta = \dot{\varepsilon}_z = 0,$$

$$R = R_0, \qquad H = H_0 \quad \text{for} \quad 1 \leq R \leq \rho_0.$$

From (2.11b) we must either set $\dot{\lambda} = 0$ or $\bar{\sigma}_r = \bar{\sigma}_\theta$. By the radial equilibrium requirement, (2.2a), and the boundary condition (2.17a), however, $\bar{\sigma}_r = \bar{\sigma}_\theta$ leads to $\bar{\sigma}_r = \bar{\sigma}_\theta = \text{constant} < 0$ which contradicts the condition $\bar{\sigma}_r \neq \bar{\sigma}_\theta$ at $R_0 = \rho_0^+$; this condition corresponds to the solution in the rigid region. We must, therefore, set $\dot{\lambda} = 0$, obtaining

$$\varepsilon_{r\theta} = 0, \qquad \theta = \theta_0,$$

where θ_0 measures angular position in the undeformed state. Hence, for the neutral regime AB, there is no plastic flow and, consequently, no strain-hardening effects. We need only to consider the stress field in the region $1 \leq R \leq \rho_0$.

To this end, we substitute from (2.18) into the yield condition (2.11a), and noting that $\bar{\sigma} = 1$ in this case, obtain

$$\bar{\sigma}_r - \bar{\sigma}_\theta = -(1 - m^2 R^{-2n-4})^{\frac{1}{2}}, \tag{3.4}$$

where the negative sign on the right side assures that $\bar{\sigma}_r$ and $\bar{\sigma}_\theta$ are continuous across the section $R = \rho_0$. Substituting (3.4) into the equilibrium equation (2.2a), setting $R = R_0$, $H = H_0 = R_0^n$, and using the continuity of the radial stress $\bar{\sigma}_r$ at $R = \rho_0$, we finally arrive at

$$\bar{\sigma}_r = -\frac{1}{\beta - n}(1 - m^2 \rho_0^{-2n-4})^{\frac{1}{2}} \left(\frac{\rho_0}{R_0}\right)^n - R_0^{-n} G(n, R_0, \rho_0) \tag{3.5a}$$

which, with the aid of (3.4), yields

$$\bar{\sigma}_\theta = \bar{\sigma}_r + (1 - m^2 R_0^{-2n-4})^{\frac{1}{2}}, \tag{3.5b}$$

where

$$G(n, R_0, \rho_0) = \int_{R_0}^{\rho_0} \xi^{n-1}(1 - m^2 \xi^{-2n-4})^{\frac{1}{2}}\, d\xi. \tag{3.5c}$$

We note that $\bar{\sigma}_{r\theta}$ is given by (2.18).

From (3.5a) and (2.17a), we obtain

$$P(t) = \frac{1}{\beta - n}(1 - m^2 \rho_0^{-2n-4})^{\frac{1}{2}} \rho_0^n + G(n, 1, \rho_0) \tag{3.6}$$

which relates ρ_0 to the load parameters $P(t)$ and $m(t)$.

In obtaining the results presented above, we have tacitly assumed that

$$m(t) \leq 1, \tag{3.7a}$$

and

$$m(t) \leq \rho_0^{n+2}, \tag{3.7b}$$

which are required in order to render all the involved physical quantities real; note that, only for $n > -2$, (3.7a) implies (3.7b). We now examine the constraint (2.15) which must be fulfilled if the state of stress is to stay on the regular regime AB. The material element at $R_0 = \rho_0$ is in the state of stress corresponding to the point D in Fig. 1, while the stress-state for an element at $R_0 = 1$ is defined by a point located somewhere between D and B. When the applied loads are such that (3.7a) is satisfied and $n > -2$, the state of stress at $R_0 = 1$ is at the corner B of the yield hexagon when $\bar{\sigma}_r(1) = -\frac{1}{2} - \frac{1}{2}(1 - m^2)^{\frac{1}{2}}$, as can be seen from (2.12a), (3.7) and (3.4). Because of the boundary condition (2.17a), the region $1 \leq R_0 \leq \rho_0$ remains in the state of stress corresponding to the regular regime AB if

$$P(t) < \tfrac{1}{2}[1 + (1 - m^2)^{\frac{1}{2}}]. \tag{3.8}$$

The domain bounded by the curve Γ_2 and the P- m-axes in Fig. 2 corresponds to (3.7a) and (3.8). The region $1 \leq R_0 \leq \rho_0(t)$ is in the neutral plastic state, corresponding to the regime AB, as long as the restrictions (3.7) and (3.8) are not violated anywhere in this region. Upon further loading, either (3.8) or (3.7) may first be violated, and, hence, two different plastic solutions, which will be called plastic solutions I and II, respectively, must now be considered.

A. *Plastic solution I*

(a) *General formulation.* When the load parameters $P(t)$ and $m(t)$ are increased in such a manner that the inequality (3.8), but not (3.7), is violated, there develops a new plastic region $\bar{b} \leq R \leq \rho_1$ corresponding to the singular regime B (Fig. 1), where $\rho_1(t)$ is the radius of the interface between the plastic region corresponding to the regime AB and that pertaining to the corner B of the Tresca's yield hexagon. The stress field in the rigid region $R = R_0 \geq \rho_0$ is given by (2.18) and (2.20) with A defined by (3.2), and that in the neutral plastic region $\rho_1 \leq R_0 \leq \rho_0$ is furnished by (2.18) and (3.5), where ρ_0 remains to be determined.

In the new plastic region $\bar{b} \le R \le \rho_1$, $\bar{\sigma}_{r\theta}$ is given by (2.18). Substituting (2.18) into (2.12a), and solving the resulting equations for $\bar{\sigma}_r$ and $\bar{\sigma}_\theta$, we obtain

$$\bar{\sigma}_r = -\frac{\bar{\sigma}}{2} - \tfrac{1}{2}(\bar{\sigma}^2 - m^2 H^{-2} R^{-4})^{\frac{1}{2}}, \tag{3.9a}$$

$$\bar{\sigma}_\theta = -\frac{\bar{\sigma}}{2} + \tfrac{1}{2}(\bar{\sigma}^2 - m^2 H^{-2} R^{-4})^{\frac{1}{2}}. \tag{3.9b}$$

With the aid of (3.9), the equilibrium equation (2.2a) may now be integrated, yielding

$$H\bar{\sigma} = D/(2DR^2 - m^2)^{\frac{1}{2}}, \tag{3.10a}$$

where $D = D(t)$ is determined from the requirement that $H = H_0$ and $\bar{\sigma} = 1$ at $R = \rho_1$, i.e.

$$D^2 - 2\rho_1^{2n+2} D + m^2 \rho_1^{2n} = 0 \tag{3.10b}$$

which yields

$$D = \rho_1^n [\rho_1^{n+2} + (\rho_1^{2n+4} - m^2)^{\frac{1}{2}}]. \tag{3.10c}$$

From (3.10a) and (3.9) we now obtain

$$\bar{\sigma}_r = -\bar{\sigma}(1 - m^2/2DR^2), \tag{3.11a}$$

$$\bar{\sigma}_\theta = -\bar{\sigma} m^2/2DR^2. \tag{3.11b}$$

The relation between ρ_0 and ρ_1 is found from the continuity of the radial stress $\bar{\sigma}_r$ at $R = \rho_1$. From (3.5a) and (3.9a) we now obtain

$$1 + (1 - m^2 \rho_1^{-2n-4})^{\frac{1}{2}} - \frac{2}{\beta - n}(1 - m^2 \rho_0^{-2n-4})^{\frac{1}{2}} (\rho_0/\rho_1)^n - 2\rho_1^{-n} G(n, \rho_1, \rho_0) = 0, \tag{3.12}$$

where the fact that $\bar{\sigma} = 1$ and $H = H_0$ for $R = \rho_1$ is also used. Equations (3.11a), (3.10a) and the boundary condition (2.17a) now relate P to ρ_1 as

$$P = (2D\bar{b} - m^2)^{\frac{1}{2}}/2\bar{b}^2, \tag{3.13}$$

where the dimensionless current radius of the hole, $\bar{b}$, remains to be determined from the displacement field.

Taking the time-derivative of both sides of equation (3.10a) and using (2.3) and (2.4), we obtain

$$\dot{\varepsilon}_z = -\frac{\dot{\bar{\sigma}}}{\bar{\sigma}} + \frac{\dot{D}}{D} - (\dot{D}R^2 - m\dot{m} + 2DR^2\dot{\varepsilon}_\theta)(2DR^2 - m^2)^{-1}. \tag{3.14}$$

Substitution from (3.11) into (2.12b) yields

$$\dot{\varepsilon}_r = \frac{\dot{\lambda}}{2}\bar{\sigma}[-1 + (1+\gamma)m^2/2DR^2], \tag{3.15a}$$

$$\dot{\varepsilon}_\theta = \frac{\dot{\lambda}}{2}\bar{\sigma}[\gamma - (1+\gamma)m^2/2DR^2], \tag{3.15b}$$

$$\dot{\varepsilon}_z = \frac{\dot{\lambda}}{2}\bar{\sigma}(1-\gamma). \tag{3.15c}$$

Equation (3.14) may now be substituted into the plastic incompressibility condition which, with the aid of (2.4), yields

$$\frac{\partial V_r}{\partial R}-\frac{m^2}{2DR^2-m^2}\frac{V_r}{R}=\frac{\dot{\bar{\sigma}}}{\bar{\sigma}}-\frac{\dot{D}}{2D}+\frac{\dot{D}m^2/2D-m\dot{m}}{2DR^2-m^2}. \tag{3.16}$$

Substitution for $\dot{\varepsilon}_\theta$ from (3.15b), and for $\dot{\varepsilon}_z$ from (3.15c) into (3.14) now results in

$$\dot{\lambda}\bar{\sigma}\frac{\dot{D}R^2-m^2}{2DR^2-m^2}=-\frac{\dot{\bar{\sigma}}}{\bar{\sigma}}+\frac{\dot{D}}{2D}-\frac{\dot{D}m^2/2D-m\dot{m}}{2DR^2-m^2}$$

which, with the aid of the hardening law (2.16), yields

$$\frac{\dot{\lambda}}{2}\bar{\sigma}=\frac{1}{a}\frac{\dot{\bar{\sigma}}}{\bar{\sigma}}=\frac{\dot{D}/D(DR^2-m^2)+m\dot{m}}{2(DR^2-m^2)+a(2DR^2-m^2)}. \tag{3.17}$$

Now we replace ε_θ by V_r/R and solve for γ from (3.15b), obtaining

$$\gamma=\frac{m^2+(4D/\dot{\lambda}\bar{\sigma})RV_r}{2DR^2-m^2}. \tag{3.18}$$

Equations (3.16–18) govern the variations of V_r, $\bar{\sigma}$, $\dot{\lambda}$ and γ.

Noting that $V_r=0$ at $R=\rho_1$ and using (3.10c), we integrate (3.16) with respect to R from R to ρ_1, at a fixed t, to obtain

$$\dot{R}=V_r=(2DR)^{-1}(2DR^2-m^2)^{\frac{1}{2}}I, \tag{3.19}$$

where

$$\begin{aligned}I=&-\frac{\dot{D}}{2D(1+a)}[(2DR^2-m^2)^{\frac{1}{2}}-D\rho_1^{-n}]-\left(\frac{\dot{D}m^2}{2D}-m\dot{m}\right)[(2DR^2-m^2)^{-\frac{1}{2}}-\rho_1^n/D]\\&+\frac{a\dot{m}-a\dot{D}m/2(1+a)D}{2(1+a)^{\frac{1}{2}}}\ln\frac{[(1+a)^{\frac{1}{2}}(2DR^2-m^2)^{\frac{1}{2}}-m][(1+a)^{\frac{1}{2}}D\rho_1^{-n}+m]}{[(1+a)^{\frac{1}{2}}(2DR^2-m^2)^{\frac{1}{2}}+m][(1+a)^{\frac{1}{2}}D\rho_1^{-n}-m]}.\end{aligned} \tag{3.20}$$

From (2.4), (2.12b) and (2.18), we have

$$R\frac{\partial}{\partial R}\left(\frac{V_\theta}{R}\right)=\frac{\dot{\lambda}}{2}(1+\gamma)m/HR^2. \tag{3.21}$$

Now, substituting (3.17), (3.18) and (3.10a) into (3.21), we integrate the resulting equation with respect to R from R to ρ_1, and using the condition that $V_\theta(R=\rho_1)=0$, arrive at

$$\begin{aligned}\dot{\theta}=\frac{V_\theta}{R}=&\frac{m\rho_1^n}{2D}\left\{-\frac{m\dot{m}}{D}+\frac{1}{1+a}\frac{\dot{D}}{D}[(\rho_1/\rho_0)^2+am^2/2D]\right\}(-R^{-2}+\rho_1^{-2})\\&+[\dot{m}-a\dot{D}m/2(1+a)D][(2DR^2-m^2)^{\frac{1}{2}}/2DR^2-\tfrac{1}{2}\rho_1^{-n-2}]\\&+\left[\frac{\dot{m}}{m}-a\dot{D}/2(1+a)D\right](1+a-am^2/2DR^2)\frac{1}{2(1+a)^{\frac{1}{2}}}\\&\times\ln\frac{[(1+a)^{\frac{1}{2}}(2DR^2-m^2)^{\frac{1}{2}}-m][(1+a)^{\frac{1}{2}}D\rho_1^{-n}+m]}{[(1+a)^{\frac{1}{2}}(2DR^2-m^2)^{\frac{1}{2}}+m][(1+a)^{\frac{1}{2}}D\rho_1^{-n}-m]}.\end{aligned} \tag{3.22}$$

(b) *Solution for a general loading program.* A general loading program may be approximated in the plane of the load parameters, P and m, by a piecewise linear path. On the ith segment of this path with the end points (m_i, P_i) and (m_{i+1}, P_{i+1}), we set

$$\dot{P} = \mu_i \dot{m}, \tag{3.23}$$

where μ_i is a non-negative constant.

Taking the time-derivative of (3.13), we have

$$\dot{D} = 2(\dot{P} + \dot{\bar{b}}/\bar{b})(2D\bar{b}^2 - m^2)^{\frac{1}{2}} - D\dot{\bar{b}}/\bar{b} + m\dot{m}\bar{b}^{-2} \tag{3.24}$$

which, in view of (3.10c) and (3.21), expresses $\dot{\rho}_1$ as a linear function of $\dot{P}$ and $\dot{m}$ with coefficients depending on the current state. If we identify the time parameter with either P or m and use (3.23), we obtain, from (3.17), (3.19), (3.22), (3.24) and (3.19) with $R = \bar{b}$, a system of first-order quasilinear differential equations for the dependent variables $\bar{\sigma}(R, t)$, $R(t)$, $\theta(R, t)$, $\rho_1(t)$ and $\bar{b}(t)$, where the coefficients in this system of equations depend on R and $\bar{b}$. For each element located at (R_0, θ_0) in the undeformed state of the disk, we can define a time t_0 at which its state of stress reaches the corner B of the yield hexagon and $R(t_0) = R_0 = \rho_1(t_0)$, $\theta(R, t_0) = \theta_0$, $\bar{b} = \bar{b}(t_0)$, $m = m(t_0)$ and $P = P(t_0)$. Then, we may employ the standard method of numerical integration, for instance the Runge–KuttaGill method [12], to solve this initial value problem. The thickness profile and the stress field are then calculated according to (3.10a), (2.18) and (3.11).

For a workhardening material, the material properties at a deformed state depend on the strain history, and, hence, the integration of (3.19) and (3.22) in a closed form is not, in general, possible. We, therefore, must employ a numerical approach.

(c) *Solution for perfectly plastic materials.* For perfectly plastic materials we have $a = 0$ and $\bar{\sigma} = 1$. Thus, with the aid of (3.10b), we reduce (3.19) to

$$[(2DR^2 - m^2)^{\frac{1}{2}}]^{\cdot} = (D\rho_1^{-n})^{\cdot} - \frac{2}{n+2}(\rho_1^{n+2})^{\cdot} \tag{3.25}$$

which may now be integrated with respect to t, yielding

$$R = (2D)^{-\frac{1}{2}}\left[\rho_1^{2n+4} + \frac{2}{n+2}(\rho_1^{2n+4} - m^2)^{\frac{1}{2}}(n\rho_1^{n+2} + 2R_0^{n+2}) + \left(\frac{n}{n+2}\rho_1^{n+2} + \frac{2}{n+2}R_0^{n+2}\right)^2\right]^{\frac{1}{2}}, \tag{3.26}$$

where the conditions that $R(t_0) = R_0$ and $\rho_1(t_0) = R_0$ are imposed, and (3.10b) is used. Moreover, setting $\bar{\sigma} = 1$, and substituting (3.26) into (3.10a), we obtain

$$H = D[(\rho_1^{2n+4} - m^2)^{\frac{1}{2}} + \frac{1}{n+2}(n\rho_1^{n+2} + 2R_0^{n+2})]^{-1}. \tag{3.27}$$

From (3.26) and (3.13), we then relate $P(t)$ to $\rho_1(t)$ as

$$\begin{aligned} P(t) = D\left[(\rho_1^{2n+4} - m^2)^{\frac{1}{2}} + \frac{1}{n+2}(n\rho_1^{n+2} + 2)\right]\Bigg[\rho_1^{2n+4} + 2(\rho_1^{2n+4} - m^2)^{\frac{1}{2}} \\ \times \frac{1}{n+2}(n\rho_1^{n+2} + 2) + \left(\frac{n}{n+2}\rho_1^{n+2} + \frac{2}{n+2}\right)^2\Bigg]^{-1}. \end{aligned} \tag{3.28}$$

Although the expression for $\dot{\theta}$ in (3.22) can be simplified for a perfectly plastic material, the direct integration with respect to t is still not possible and a numerical integration is required; this reveals the fact that the angular displacement is a path-dependent quantity.

(d) *Conditions assuring the validity of solution.* In addition to the restriction (2.13), which assures that the stress-state remains in the singular regime B (Fig. 1), we must consider the following conditions

$$2D\bar{b}^2 > m^2, \tag{3.29a}$$

$$m < \rho_1^{n+2}, \tag{3.29b}$$

which are required in order to render all the physical quantities real. In view of (3.13), (3.29a) is fulfilled if $P(t) > 0$, but (3.29b) may still restrict the admissible values of P and m. In view of (3.10c) and (3.28), for non-hardening materials, this restriction takes on the form

$$P > \frac{m^{(2n+2)/(n+2)}}{m^2+(nm+2)/(n+2)}. \tag{3.30}$$

The corresponding form for hardening materials cannot be obtained explicitly and must be imposed in the course of the numerical integration.

From (3.10c) and (3.29b), it can be shown that

$$D\rho_1^2 - m^2 > 0 \tag{3.31}$$

which, together with (3.17) and (3.29b), shows that the condition $\dot{\lambda} > 0$ is satisfied at $R = \rho_1$. To see the implication of $\dot{\lambda} > 0$ in the region $\bar{b} \leq R \leq \rho_1$, we rewrite $\dot{\lambda} > 0$ and (3.17) in the form

$$\frac{1}{1+a}\frac{\dot{D}}{2D} + \left(m\dot{m} - \frac{a}{1+a}\frac{\dot{D}m^2}{2D}\right)\frac{1}{(1+a)(2DR^2-m^2)-m^2} > 0, \tag{3.32}$$

for $\bar{b} \leq R \leq \rho_1, \dot{m} \geq 0$ and $\dot{D} > 0$. Now, to satisfy (3.32), the quantity $(1+a)(2DR^2-m^2)-m^2$ must not change sign for the values of R between $\bar{b}$ and ρ_1. Therefore, because of (3.31), we must have

$$(1+a)[2D\bar{b}^2 - m^2] - m^2 > 0. \tag{3.33}$$

If (3.29a) and $\dot{\lambda} > 0$ are fulfilled, it can be seen from (3.18) that $\gamma > 0$ is automatically satisfied. We can express the condition implied by $\gamma \leq 1$ in terms of the rates of the field quantities, using (3.17) and (3.18). For non-hardening materials, this leads to

$$\dot{D}(2D\bar{b}^2 - m^2)^{\frac{1}{2}} \geq \rho_1^n(\dot{D}\rho_1^2 - m\dot{m}). \tag{3.34}$$

The equality in (3.34) for non-hardening materials, or in general when $\gamma = 1$, causes a new plastic region to develop at the vicinity of the hole; this plastic region corresponds to the regular regime AB and has the flow rule (2.11b). We note that, since $\dot{\varepsilon}_z = 0$ in this new plastic region, the thickness at each element remains at the same value that it had reached at the end of the solution corresponding to the singular regime B.

B. *Plastic solution II*

We now consider the solution for $m > 1$ which violates (3.7a). First we observe that when $m > 1$, equation (3.4) (which pertains to the neutral plastic region) does not remain valid if the hole's radius stays at its initial value b_0. We must, therefore, consider a new

plastic region, $\bar{b} \leq R \leq \rho_1$, at the vicinity of the hole that corresponds to the regime $A'B'$ of the yield hexagon (Fig. 1). The solution for the rigid region $R > \rho_0$ is given by (2.18), (2.17) and (3.2), and that in the neutral plastic region $\rho_1 \leq R \leq \rho_0$ is given by (2.18) and (3.5), where ρ_0 and ρ_1 are as yet to be determined.

In the new plastic region $\bar{b} \leq R \leq \rho_1$, (3.3) is still valid and the continuity of V_r at $R = \rho_1$ requires that $V_r = 0$ for $\bar{b} \leq R \leq \rho_1$. Thus, from (2.4) and (2.11b), we have

$$\dot{\varepsilon}_r = \dot{\varepsilon}_\theta = \dot{\varepsilon}_z = 0, \qquad R = R_0, \qquad H = H_0 = R_0^n, \tag{3.35a}$$

and, hence, the considered region is characterized by

$$\bar{\sigma}_r = \bar{\sigma}_\theta, \qquad \dot{\lambda} > 0, \qquad \dot{\varepsilon}_{r\theta} \neq 0. \tag{3.35b}$$

Since in this region no radial displacement takes place, $\bar{\sigma}_{r\theta}$ is given by (2.18). Substituting (3.35b) into (2.11a), we have

$$\bar{\sigma} = 2\bar{\sigma}_{r\theta} = mR_0^{-n-2}, \quad \text{for} \quad 1 \leq R_0 \leq \rho_1. \tag{3.36}$$

Now, with the aid of (3.35) and the boundary condition (2.17a), the equilibrium equation (2.2a) can be solved, yielding

$$\bar{\sigma}_r = \bar{\sigma}_\theta = -PR_0^{-n}. \tag{3.37}$$

Setting $R_0 = \rho_1$ in (3.35b) and (3.4), we relate ρ_1 to m as

$$m = \rho_1^{n+2}. \tag{3.38}$$

From (3.5a), (3.37) and the continuity of $\bar{\sigma}_r$ at $R = \rho_1$, we obtain

$$P = \frac{1}{\beta - n}\rho_0^n\left[1 - \left(\frac{\rho_1}{\rho_0}\right)^{2n+4}\right]^{\frac{1}{2}} + G(n, \rho_1, \rho_0) \tag{3.39}$$

which relates ρ_0 and P. In (3.39), the function G is defined by (3.5c).

Substituting (3.36) into the hardening law (2.16), we obtain

$$\frac{\dot{\lambda}}{2} = \frac{\dot{m}}{am^2}R_0^{n+2} \tag{3.40a}$$

which, with the aid of (2.11b), (2.18) and (3.38), now yields

$$\dot{\varepsilon}_{r\theta} = \frac{n+2}{a}\frac{\dot{\rho}_1}{\rho_1}. \tag{3.40b}$$

Equation (3.40b) and the relation (2.4) then give

$$\frac{\partial}{\partial R_0}\left(\frac{V_\theta}{R_0}\right) = \frac{2(n+2)}{a}\frac{1}{R_0}\frac{\dot{\rho}_1}{\rho_1} \tag{3.40c}$$

which, with the condition that $V_\theta(R_0 = \rho_1) = 0$, can be integrated with respect to R_0, yielding

$$\dot{\theta} \equiv \frac{V_\theta}{R_0} = \frac{2(n+2)}{a}\frac{\dot{\rho}_1}{\rho_1}\ln\left(\frac{R_0}{\rho_1}\right). \tag{3.40d}$$

Treating ρ_1 as our time parameter, and noting that $\theta = \theta_0$ at $\rho_1 = R_0$, we can integrate (3.40d) to obtain

$$\theta = \theta_0 - \frac{n+2}{a}\left(\ln\frac{R_0}{\rho_1}\right)^2 \tag{3.41}$$

which also indicates that the solution given in this section is valid only for hardening materials, $a > 0$.

Because of (3.40a), the restriction $\dot{\lambda} > 0$ is always fulfilled if $\dot{m} > 0$. From (3.35b), the restriction (2.15) requires that $|\bar{\sigma}_r| < \bar{\sigma}_{r\theta}$ for $1 \leq R_0 \leq \rho_1$ which, in view of (3.36–38), yields

$$P < \tfrac{1}{2}m^{n/(n+2)}. \tag{3.42}$$

When the condition (3.42) is first violated (with an equality sign), it can be shown from (3.37) and (3.38) that at $R_0 = \rho_1$, $\bar{\sigma}_{r\theta} = -\bar{\sigma}_r$, $\bar{\sigma}_1 = 0$ and $\bar{\sigma}_2 = -2\bar{\sigma}_{r\theta} < 0$; this state of stress corresponds to the singular regime B' of the yield hexagon (Fig. 1). For $P > \frac{1}{2}m^{n/(n+2)}$, there exists a new plastic region, $\rho_2 \leq R \leq \rho_1$, in which the state of stress is at the regime B': this new plastic region bounds the inner region $\bar{b} \leq R \leq \rho_2$ at $R = \rho_2$. The solutions for the regions $\rho_2 \leq R \leq \rho_1$, $\rho_1 \leq R_0 \leq \rho_0$ and $R_0 \geq \rho_0$ are essentially the same as those considered in the last section; the functional relations among ρ_1, ρ_2, P and m, must, of course, be determined.

In the region $\bar{b} \leq R \leq \rho_2$, the state of stress is on the regime AB, where no thickening takes place. We thus must have

$$RV_r \equiv R\dot{R} = \dot{e}(t) = \rho_2 V_r(R = \rho_2). \tag{3.43a}$$

We denote by t_0 the instant at which this region is initiated, where $e(t_0) = 0$, $R(t_0) = R_0$ and $\rho_1(t_0) = \rho_2(t_0) = \rho_{10}$; for $t > t_0$, $\rho_1 > \rho_2$. Then, we integrate (3.43a) with respect to t from t_0 to t, obtaining

$$R^2 = R_0^2 + 2e(t), \tag{3.43b}$$

$$e(t) = \int_{t_0}^{t} \rho_2 V_r(R = \rho_2)\,\mathrm{d}t, \tag{3.43c}$$

where $V_r(R = \rho_2)$ is given by (3.19). Since $\dot{\varepsilon}_z = \dot{H}/H = 0$ implies that $H = H_0$, from (3.43b) we have

$$H = (R^2 - 2e)^{n/2} \tag{3.44}$$

which can then be substituted into (2.18) to yield

$$\bar{\sigma}_{r\theta} = \frac{m}{2}R^{-2}(R^2 - 2e)^{-n/2}. \tag{3.45a}$$

An equation governing $\dot{\theta}$ is then obtained from (2.3), (2.4), (2.11) and (3.43) as

$$\frac{\partial\dot{\theta}}{\partial R} = \dot{e}R^{-3}\frac{4\bar{\sigma}_{r\theta}}{(\bar{\sigma}^2 - 4\bar{\sigma}_{r\theta}^2)^{\frac{1}{2}}}, \tag{3.45b}$$

where $\bar{\sigma}_{r\theta}$ is given by (3.45a). Now, we can eliminate H, $\bar{\sigma}_\theta$ and $\bar{\sigma}_{r\theta}$ from (2.2a), (2.11a), (3.44) and (3.45a), integrate the resulting equation, and using the boundary condition (2.17a), obtain

$$\bar{\sigma}_r = -PR_0^{-n} + R_0^{-n}\int_{\bar{b}}^{R} \frac{1}{y}(y^2 - 2e)^{n/2}[\bar{\sigma}^2 - m^2 y^{-4}(y^2-2e)^{-n}]^{\frac{1}{2}}\,dy \tag{3.46a}$$

and

$$\bar{\sigma}_\theta = \bar{\sigma}_r + [\bar{\sigma}^2 - m^2 R^{-4}(R^2-2e)^{-n}]^{\frac{1}{2}}. \tag{3.46b}$$

Moreover, from (2.4), (2.11b), (2.5), (3.43a) and (3.46), we have

$$\dot{\bar{\sigma}} = \dot{e}a\bar{\sigma}^2[\bar{\sigma}^2 R^4 - m^2(R^2-2e)^{-n}]^{-\frac{1}{2}} \tag{3.47a}$$

which is the equation governing $\dot{\bar{\sigma}}$ subject to the condition

$$\bar{\sigma}(R, t = t_0) = m(t = t_0)R_0^{-n-2} \tag{3.47b}$$

given by (3.36). Setting $R = \rho^2$ in (3.10a) and using (3.43b) and (3.44), we obtain

$$\bar{\sigma}(R = \rho^2) = D(2D\rho_2^2 - m^2)^{-\frac{1}{2}}(\rho_2^2 - 2e)^{-n/2}, \tag{3.48}$$

where D is given by (3.10c) as a function of ρ_1 and m. From (3.11a), (3.46a) and (3.48), the continuity of $\bar{\sigma}_r$ at $R = \rho_2$ now yields

$$P = \tfrac{1}{2}\rho_2^{-2}(2D\rho_2^2 - m^2)^{\frac{1}{2}} + \int_{\bar{b}}^{\rho_2} [\bar{\sigma}^2 y^{-2}(y^2-2e)^n - m^2 y^{-6}]^{\frac{1}{2}}\,dy. \tag{3.49}$$

Taking the derivative of (3.49) and using (3.43), (3.47a) and (3.48), we have

$$\begin{aligned}\dot{P} = {} & \{g_1(\bar{b}, \rho_2) - \bar{b}^{-4}[\bar{b}^4\bar{\sigma}^2(\bar{b}) - m^2]^{\frac{1}{2}}\}\dot{e} + \tfrac{1}{2}(2D\rho_2^2 - m^2)^{-\frac{1}{2}}\dot{D} \\ & - [g_2(\bar{b}, \rho_2) + \tfrac{1}{2}\rho_2^{-2}(2D\rho_2^2 - m^2)^{-\frac{1}{2}}]m\dot{m},\end{aligned} \tag{3.50a}$$

where

$$g_1(\bar{b}, \rho_2) = \int_{\bar{b}}^{\rho_2} \{-y^{-5}[g_3(y)]^{\frac{1}{2}} + 2m^2 y^{-5}[g_3(y)]^{-\frac{1}{2}} + a\bar{\sigma}^3 y(y^2-2e)^{3n/2}[g_3(y)]^{-1}\}\,dy, \tag{3.50b}$$

$$g_2(\bar{b}, \rho_2) = \int_{\bar{b}}^{\rho_2} y^{-3}[g_3(y)]^{-\frac{1}{2}}\,dy, \tag{3.50c}$$

and where

$$g_3(R) = \bar{\sigma}^2 R^4(R^2-2e)^n - m^2. \tag{3.50d}$$

For the numerical calculation, it is convenient to consider ρ_1 as our time parameter. With the aid of (3.10c), the rate quantities $\dot{e}$, $\dot{P}$ and $\dot{m}$ at a given state and for a general loading program can be obtained from (3.23), (3.50), (3.43a) and (3.19). With $\dot{e}$ known, $\dot{\bar{\sigma}}$ follows from (3.47) and $\dot{\theta}(R, \rho_1)$ for $\bar{b} \le R < \rho_2$ can be obtained from (3.45b) with the boundary condition $\dot{\theta}(\rho_2, \rho_1)$ given by (3.22) for $R = \rho_2$. From these rate quantities, we can now solve for the field quantities at a new state; due to the fact that the coefficient of $\dot{\rho}_2$ in (3.50a) is identically zero, the values of ρ_2 at this new state cannot be calculated directly and have to be evaluated from the condition (3.48) which must be satisfied at $R = \rho_2$.

For the special loading program

$$m = m_0 = \text{constant} = m(t_0), \tag{3.51}$$

we can relate $\bar{\sigma}(R, \rho_1)$ to $e(\rho_1)$ and $\rho_2(\rho_1)$ to ρ_1 implicitly, where ρ_1 is considered as the time parameter. Indeed, for the loading program (3.51) and in view of (3.43b), (3.47) can be integrated to yield

$$[a\bar{\sigma}(R_0^2+2e)+2g(\bar{\sigma}, e)]^{a^2}[\bar{\sigma}(R_0^2+2e)+g(\bar{\sigma}, e)]^{-2a}\bar{\sigma}^{-a^2+4} = a^{a^2}m_0^{-2(a-2)}R_0^{2(a-2)(a+n+2)}, \quad \text{for } a \neq 2, \tag{3.52a}$$

and

$$\bar{\sigma}(R_0^2+2e)+g(\bar{\sigma}, e) = m_0^{-1}\bar{\sigma}^2R_0^{n+4}\exp\left[\frac{g(\bar{\sigma}, e)}{\bar{\sigma}(R_0^2+2e)+g(\bar{\sigma}, e)}\right] \quad \text{for } a = 2, \tag{3.52b}$$

where

$$g(\bar{\sigma}, e) = [\bar{\sigma}^2(R_0^2+2e)^2 - m_0^2R_0^{-2n}]^{\frac{1}{2}}. \tag{3.52c}$$

Setting $R_0^2 = \rho_2^2 - 2e$, we obtain, from (3.48) and (3.52),

$$[(a+2)D\rho_2^2 - 2m_0^2]^{a^2}[2D\rho_2^2 - m_0^2]^{-a-2}(\rho_2^2-2e)^{-a^2+4} = D^{a^2-4}a^{a^2}m_0^{-2(a-2)}, \quad \text{for } a \neq 2, \tag{3.53a}$$

and

$$m_0(2D\rho_2^2 - m_0^2)^{3/2}(\rho_2^2-2e)^{-2} = D^2\exp[1 - D\rho_2^2(2D\rho_2^2 - m_0^2)^{-1}], \quad \text{for } a = 2, \tag{3.53b}$$

where D as a function of ρ_1 is defined by (3.10c) with $m = m_0$.

C. *Discussion and numerical results*

As can be seen from the results of subsection $A-(c)$ of the present section, the angular change $\theta-\theta_0$ in an active plastic state depends on the strain history even for a perfectly plastic material ($a = 0$). For workhardening materials, the solution in an active plastic state must be obtained by tracing the strain history. For this purpose, we have expressed the governing equations in the form of a system of first-order quasilinear differential equations, reducing the problem to an initial value problem which can be solved readily by a numerical method [12].

Figure 3(a) is the plot of the radial displacement $u_r/b_0 = U_r$ at the hole as a function of the pressure parameter P for the indicated values of m and a, and for an initially uniform disk ($n = 0$); the values of the work-hardening parameter a are taken to be 0, 0·1, 0·5, 1 and 5, and for each value of a, the values of twisting parameter m are taken to be 0, 0·5 and 1. The corresponding results for an initially conical disk ($n = 1$) are shown in Fig. 3(b). We note that the results in Fig. 3(a), for $n = 0$ and $a = 0$, are also given in [10]. From Figs. 3(a) and (b), we observe that, for given values of P and m, the radial displacement $U_r(b)$ decreases with an increase in the workhardening parameter a, and increases with an increase in the twisting parameter m for fixed values of P and a.

We next consider the solutions corresponding to the state $m = 1$ and $P = 1{\cdot}5$, being attained by the three loading paths (a), (b) and (c) which are shown in Fig. 2. Figure 4 shows the thickness distribution for $n = 0$ and $n = 1$, and $a = 0$, 0·1 and 1; the results for the paths (a), (b) and (c) are shown by solid, dashed and dash–dot lines, respectively. It can be seen from Fig. 4 that these three loading paths yield quite different thicknesses at the vicinity of the hole. The corresponding results for the stress fields in the active plastic region are shown in Fig. 5(a) for $n = 0$ and in Fig. 5(b) for $n = 1$. As is seen, the stress field is highly

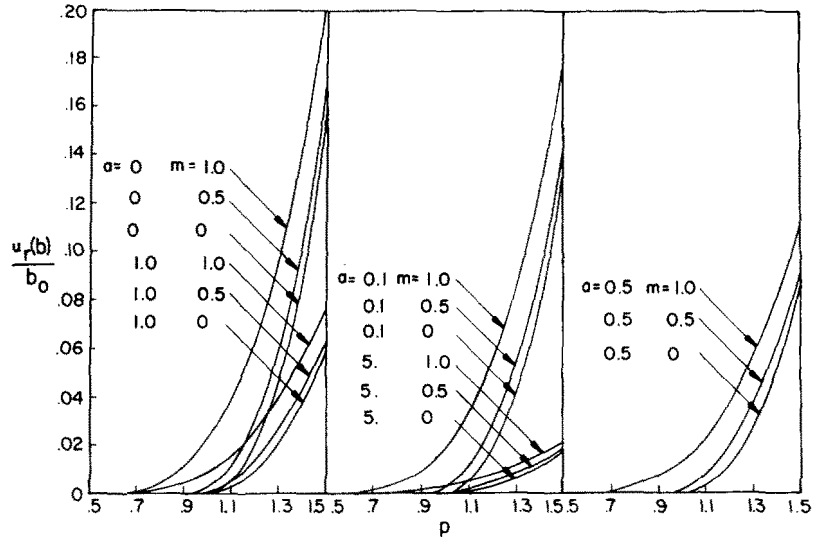

FIG. 3(a). Radial displacement at the edge of the hole for $n = 0$ and indicated values of m and a.

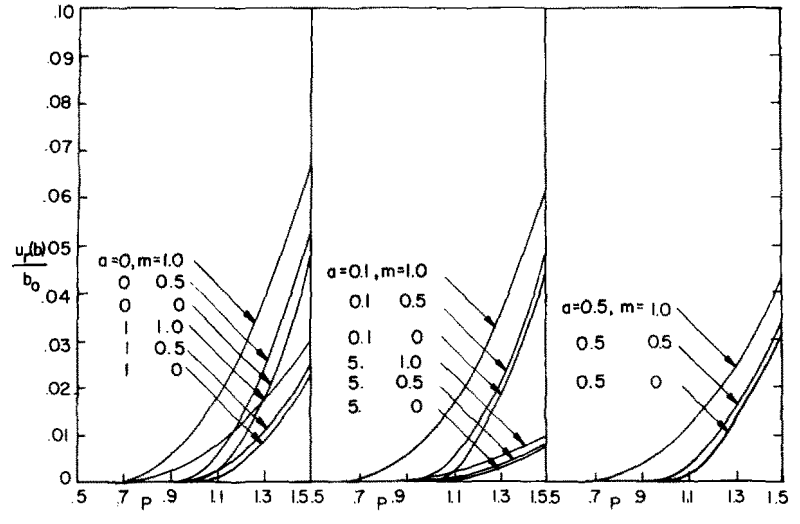

FIG. 3(b). Radial displacement at the edge of the hole for $n = 1$ and indicated values of m and a.

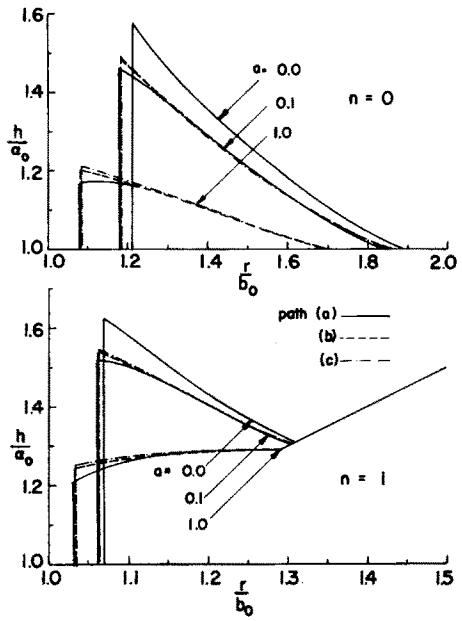

FIG. 4. Thickness distribution for $m = 1$ and $P = 1{\cdot}5$, and three loading paths shown in Fig. 2.

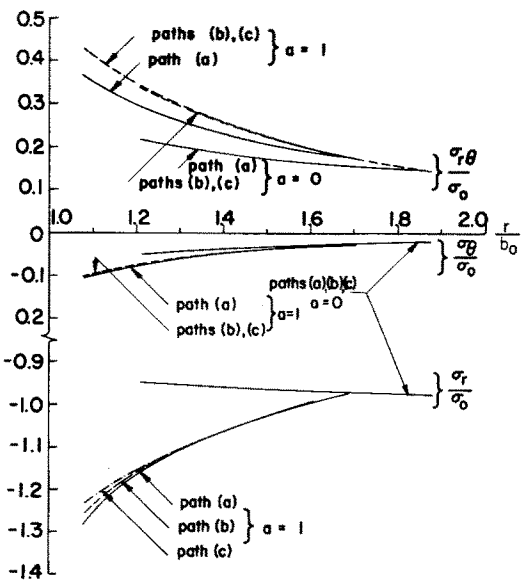

FIG. 5(a). Stress distribution for $n = 0$, $m = 1$ and $P = 1{\cdot}5$, and three loading paths shown in Fig. 2.

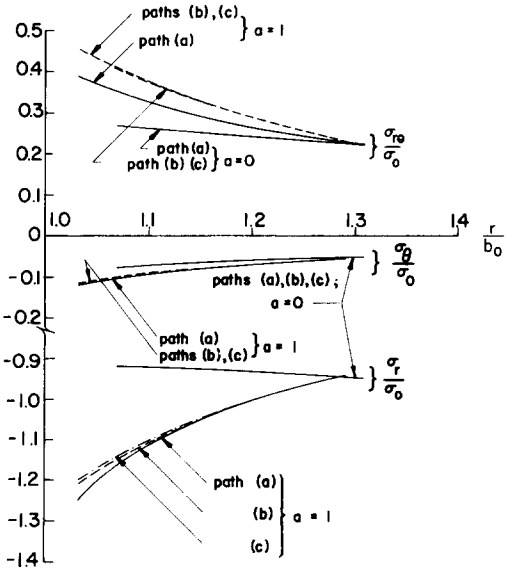

FIG. 5(b). Stress distribution for $n = 1$, $m = 1$ and $P = 1{\cdot}5$, and three loading paths shown in Fig. 2.

affected by the workhardening parameter a. For perfectly plastic materials ($a = 0$), only the component $\bar{\sigma}_{r\theta}$ is path-dependent; the distribution of $\bar{\sigma}_{r\theta}$ for path (b) cannot be distinguished in the figure from that corresponding to the path (c). For workhardening materials ($a = 1$), the components $\bar{\sigma}_{r\theta}$ and $\bar{\sigma}_\theta$ for path (b) cannot be distinguished in the figures from those for the path (c); the distributions of $\bar{\sigma}_r$ for these three paths are quite distinct. For more accurate results, we record in Table 1 the values of the radial displacement, angular displacement and thickness, all at the edge of the hole, for $n = 0$ and $n = 1$, and corresponding to the three paths (a), (b) and (c).

The angular displacement at the edge of the hole of an initially conical disk ($n = 1$) is displayed in Fig. 6 for several values of a, and $P \leq \frac{1}{2}m^{\frac{1}{3}}$. This figure again reveals the effect of the workhardening parameter, a, on the displacement field.

4. INFINITESIMAL DEFORMATION OF AN ELASTIC–PLASTIC DISK

A. *Elastic–plastic solution*

In this section we shall consider the elastic–plastic solution at the vicinity of the hole for further loading subsequent to the initiation of a plastic state at the edge of the hole; elastic strains are included and infinitesimal theory is used, hence, no distinction will be made between R and R_0, and $\bar{\alpha} = 1$. As in the last section, upon further loading that violates (2.24), there develops a plastic region $1 < R < \bar{\rho}_0$ at the vicinity of the hole, where $\bar{\rho}_0$ defines the elastic–plastic interface. In the elastic region $R \geq \bar{\rho}_0$, the displacement and stress fields are given by (2.22), (2.18) and (2.20) with A defined by (3.2) where ρ_0 must be replaced by $\bar{\rho}_0$. However, since V_r at $R = \bar{\rho}_0$ is non-zero, the neutral plastic region does not exist in the present case. The stress-state for the elastic–plastic region $1 \leq R \leq \bar{\rho}_0$ corresponds to the regime $A'B'$ of the yield hexagon, Fig. 1. To seek the solution in this region, we shall regard the yield stress $\bar{\sigma}$ as our basic unknown.

TABLE 1. VALUES OF $\left\{\frac{u_r}{b_0}, \theta-\theta_0, \frac{h}{\alpha_0}\right\}^{\dagger}$ AT $r = b$, FOR $m = 1$ AND $P = 1{\cdot}5$, AND VARIOUS LOADING PATHS SHOWN IN FIG. 2

Paths	n	a				
		0	0·1	0·5	1	5
(a)	0	0·210265	0·179076	0·112388	0·076668	0·021624
		0·133727	0·118116	0·080540	0·057605	0·017551
		1·577683	1·462343	1·259519	1·166244	1·042151
(b)	0	0·210265	0·180346	0·115277	0·079590	0·022956
		0·097274	0·086628	0·060339	0·043784	0·013724
		1·577683	1·488344	1·301083	1·203190	1·056234
(c)	0	0·210265	0·181090	0·117018	0·081387	0·023810
		0·067484	0·060228	0·042274	0·030876	0·009826
		1·577683	1·494018	1·313433	1·215376	1·061578
(a)	1	0·069041	0·061660	0·043063	0·031201	0·009693
		0·061529	0·055085	0·038856	0·028390	0·008982
		1·627605	1·514811	1·307591	1·204197	1·054902
(b)	1	0·069041	0·062149	0·044312	0·032554	0·010387
		0·042330	0·038457	0·028095	0·020980	0·006908
		1·627605	1·542607	1·350281	1·241904	1·069162
(c)	1	0·069041	0·062396	0·044984	0·033311	0·010802
		0·028789	0·026285	0·019466	0·014679	0·004931
		1·627605	1·547972	1·362299	1·253891	1·074462

† For each loading path, the first row is the value of u_r/b_0, the second is $\theta-\theta_0$ and the last is h/α_0 all at $r = b$.

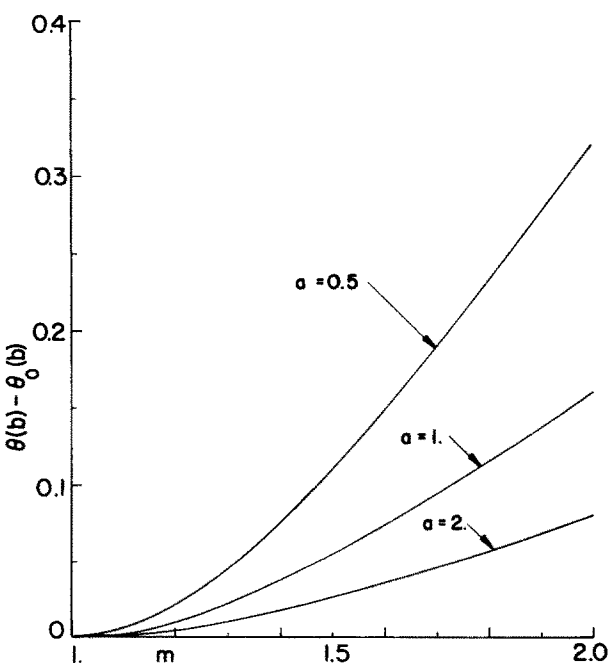

FIG. 6. Angular displacement at the edge of the hole for $n = 1$, and $P < \frac{1}{2}m^{\frac{1}{2}}$.

Substituting (2.18) into the yield condition (2.11a) we have

$$\bar{\sigma}_r - \bar{\sigma}_\theta = -\psi(\bar{\sigma}, R), \tag{4.1}$$

$$\psi(\bar{\sigma}, R) = (\bar{\sigma}^2 - m^2 R^{-2n-4})^{\frac{1}{2}}. \tag{4.2}$$

Eliminating $\bar{\sigma}_\theta$ from (2.19) and (4.1), and integrating the resulting equation subject to the boundary condition (2.17a) with $\bar{\alpha} = 1$, we obtain

$$\bar{\sigma}_r = R^{-n}\left[-P + \int_1^R y^{n-1}\psi(\bar{\sigma}, y)\,\mathrm{d}y\right]. \tag{4.3a}$$

The stress-component $\bar{\sigma}_\theta$ is now given by

$$\bar{\sigma}_\theta = \bar{\sigma}_r + \psi(\bar{\sigma}, R), \tag{4.3b}$$

and the shearing stress $\bar{\sigma}_{r\theta}$ is, of course, defined by (2.18).

From (2.20a), (3.2) and (4.3a), the continuity of $\bar{\sigma}_r$ at $R = \bar{\rho}_0$ relates $\bar{\rho}_0$ to P as

$$P = (\beta - n)^{-1}\bar{\rho}_0^n\psi(1, \bar{\rho}_0) + \int_1^{\bar{\rho}_0} y^{n-1}\psi(\bar{\sigma}, y)\,\mathrm{d}y. \tag{4.4}$$

Before we determine $\bar{\sigma}$, and subsequently ψ, as functions of R, we shall first consider the displacement field.

For the stress point on the regime $A'B'$, Fig. 1, the flow rules (2.11b) give

$$\dot{\varepsilon}_r'' + \dot{\varepsilon}_\theta'' = \dot{\varepsilon}_z'' = 0$$

which, with the initial conditions that the plastic strains are zero at the initiation of the plastic flow, yield

$$\dot{\varepsilon}_r'' + \dot{\varepsilon}_\theta'' = \dot{\varepsilon}_z'' = 0 \tag{4.5a}$$

and, thus,

$$\varepsilon_r + \varepsilon_\theta = \varepsilon_r' + \varepsilon_\theta', \tag{4.5b}$$

$$\varepsilon_z = \varepsilon_z'. \tag{4.5c}$$

Upon substitution from (2.6) and (2.7), (4.5b, c) give

$$\frac{1}{R}\frac{\mathrm{d}}{\mathrm{d}R}(RU_r) = \frac{1-\nu}{\bar{E}}(\bar{\sigma}_r + \bar{\sigma}_\theta), \tag{4.6a}$$

and

$$H = H_0\left[1 - \frac{\nu}{\bar{E}}(\bar{\sigma}_r + \bar{\sigma}_\theta)\right]. \tag{4.6b}$$

With the aid of (4.1), (4.6b) yields the thickness profile

$$\frac{H}{H_0} = 1 - \frac{\nu}{\bar{E}}[2\bar{\sigma}_r + \psi(\bar{\sigma}, R)], \tag{4.7}$$

where ψ is given by (4.2), and $\bar{\sigma}_r$ is given by (4.3a). Substituting $\bar{\sigma}_\theta$ from (2.19), we can rewrite (4.6a) as

$$\frac{\mathrm{d}}{\mathrm{d}R}(RU_r) = \frac{1-\nu}{\bar{E}}\left[nR\bar{\sigma}_r + \frac{\mathrm{d}}{\mathrm{d}R}(R^2\bar{\sigma}_r)\right]. \tag{4.8}$$

In view of (4.3a), (4.4) and the continuities of U_r and $\bar{\sigma}_r$ at $R = \bar{\rho}_0$ given by (2.22a), (2.20a) and (3.2), we may apply Fubini's theorem to the double integral, and integrate (4.8) to obtain

$$\frac{\bar{E}U_r}{R} = \left(\frac{\bar{\rho}_0}{R}\right)^2 \psi\left(1, \frac{\rho_0}{R}\right) + (1-\nu)\left\{(\beta-n)^{-1}(2-n)^{-1}\left[n\left(\frac{\bar{\rho}_0}{R}\right)^2 - 2\left(\frac{\bar{\rho}_0}{R}\right)^n\right]\psi(1, \bar{\rho}_0)\right.$$

$$\left. + (2-n)^{-1}\int_R^{\bar{\rho}_0} (nR^{-2}y - 2R^{-n}y^{n-1})\psi(\bar{\sigma}, y)\,\mathrm{d}y\right\}, \quad \text{for } n \neq 2, \tag{4.9a}$$

and

$$\frac{\bar{E}U_r}{R} = \left(\frac{\bar{\rho}_0}{R}\right)^2 \psi\left(1, \frac{\bar{\rho}_0}{R}\right) + (1-\nu)\left\{(\beta-n)^{-1}\left(\frac{\bar{\rho}_0}{R}\right)^2\left[2\ln\left(\frac{\bar{\rho}_0}{R}\right) - 1\right]\psi(1, \bar{\rho}_0)\right.$$

$$\left. + R^{-2}\int_R^{\bar{\rho}_0} y(2\ln y - 2\ln R - 1)\psi(\bar{\sigma}, y)\,\mathrm{d}y\right\}, \quad \text{for } n = 2. \tag{4.9b}$$

Since $\varepsilon_\theta'' = -\varepsilon_r'' = \varepsilon_\theta - \varepsilon_\theta'$, from (2.6) and (2.7) (without superposed dots), we have

$$\varepsilon_\theta'' = -\varepsilon_r'' = \frac{U_r}{R} - \frac{1}{\bar{E}}(\bar{\sigma}_\theta - \nu\bar{\sigma}_r)$$

which, upon substitution from (4.1), (4.3), (4.4) and (4.9), yields

$$\bar{E}\varepsilon_\theta'' = -\bar{E}\varepsilon_r'' = \left(\frac{\bar{\rho}_0}{R}\right)^2 \psi(1, \bar{\rho}_0) - \psi(\bar{\sigma}, R) + n(1-\nu)(2-n)^{-1}\left\{(\beta-n)^{-1}\left[\left(\frac{\bar{\rho}_0}{R}\right)^2\right.\right.$$

$$\left.\left. - \left(\frac{\bar{\rho}_0}{R}\right)^n\right]\psi(1, \bar{\rho}_0) + \int_R^{\bar{\rho}_0} (R^{-2}y - R^{-n}y^{n-1})\psi(\bar{\sigma}, y)\,\mathrm{d}y\right\}, \quad \text{for } n = 2, \tag{4.10a}$$

and

$$\bar{E}\varepsilon_\theta'' = -\bar{E}\varepsilon_r'' = \left(\frac{\bar{\rho}_0}{R}\right)^2 \psi(1, \bar{\rho}_0) - \psi(\bar{\sigma}, R) + 2(1-\nu)\left\{(\beta-n)^{-1}\left(\frac{\bar{\rho}_0}{R}\right)^2 \ln\left(\frac{\bar{\rho}_0}{R}\right)\psi(1, \bar{\rho}_0)\right.$$

$$\left. + R^{-2}\int_R^{\bar{\rho}_0} y(\ln y - \ln R)\psi(\bar{\sigma}, y)\,\mathrm{d}y\right\}, \quad \text{for } n = 2. \tag{4.10b}$$

It is important to note that the integral terms in (4.9) and (4.10) vanish only if $n = 0$, i.e. for a uniform disk which, of course, is a very special case of the general problem treated in the present study.

Eliminating $\dot{\lambda}$ and $\bar{\sigma}_r - \bar{\sigma}_\theta$ from (2.11), (2.16) and (4.1), we arrive at

$$\psi(\bar{\sigma}, R)\frac{\dot{\bar{\sigma}}}{a\bar{\sigma}^2} = \dot{\varepsilon}_\theta'' \tag{4.11}$$

where $\dot{\varepsilon}_\theta''$ is obtained by taking the derivative of (4.10) with respect to time parameter t, and setting $\bar{\sigma} = 1$ at $\bar{\rho}_0 = R$. At a given state, (4.11) defines the rate $\dot{\bar{\sigma}}(R, t)$.

To determine the angular displacement, we first rewrite (2.6) as

$$\frac{U_\theta}{R} = \frac{U_\theta}{R}\bigg|_{R\to\infty} - 2\int_R^\infty \frac{\varepsilon_{r\theta}}{R}\,\mathrm{d}R = -2\int_R^\infty \frac{\varepsilon_{r\theta}'}{R}\,\mathrm{d}R - 2\int_R^{\bar{\rho}_0} \frac{\varepsilon_{r\theta}''}{R}\,\mathrm{d}R.$$

From (2.7) and (2.18), for $n > -2$, we obtain

$$-2\int_R^\infty \frac{\varepsilon'_{r\theta}}{R}\,dR = -\frac{1+\nu}{\bar{E}}\frac{m}{n+2}R^{-n-2}.$$

Noting (2.11b) and (2.16), we have

$$-2\int_R^{\bar{\rho}_0} \frac{\dot{\varepsilon}''_{r\theta}}{R}\,dR = -2\int_R^{\bar{\rho}_0} \frac{m\dot{\bar{\sigma}}}{a\bar{\sigma}^2}R^{-n-3}\,dR$$

Therefore,

$$\frac{\bar{E}\dot{U}_\theta}{R} = -\frac{1+\nu}{n+2}R^{-n-2}\dot{m} - \frac{2\bar{E}m}{a}\int_R^{\bar{\rho}_0}\frac{\dot{\bar{\sigma}}}{\bar{\sigma}^2}R^{-n-3}\,dR. \tag{4.12}$$

In view of (4.11), (4.12) defines the rate of change of U_θ whose initial value at $\bar{\rho}_0 = R$ is given by (2.22b).

Upon substitution for the stresses from (2.18) and (4.3), we can rewrite the restriction $\bar{\sigma}_r\bar{\sigma}_\theta < \bar{\sigma}_{r\theta}^2$, which confines the state of stress corresponding to the regime $A'B'$ in Fig. 1, as

$$\left\{-2PR^{-n} + \psi(\bar{\sigma}, R) + 2R^{-n}\int_1^R y^{n-1}\psi(\bar{\sigma}, y)\,dy\right\}^2 < \bar{\sigma}^2. \tag{4.13}$$

The state of stress must satisfy (4.13), with the equality sign corresponding to the singular regime B' of the yield hexagon, Fig. 1. With the aid of (4.4), it is found that (4.13) is always satisfied at $R = \bar{\rho}_0$ for values of n between -2 and 2, provided that

$$m < \bar{\rho}_0^{n+2} \tag{4.14}$$

which is also required in order to render the physical quantities real. However, as noted in [11] for a uniform disk, $n = 0$, (4.13) may be first violated (with equality sign) at $R \neq 1$. We shall consider such a loading program that (4.13) is satisfied for $1 \leq R \leq \bar{\rho}_0$, since, as noted in [11], when the state of stress reaches the singular regime B', no further deformation can be predicted by the infinitesimal theory. We finally note that the condition $\dot{\lambda} > 0$ implies $\dot{\bar{\sigma}} > 0$, as can be seen from the hardening law (2.16).

Considering $\bar{\rho}_0$ as our time parameter, for a general loading program defined by

$$\dot{P} = \mu\dot{m}, \tag{4.15}$$

where μ is a given function of P and m, we may eliminate $\dot{P}$, $\dot{m}$ and $\dot{\varepsilon}''_\theta$ from (4.12), (4.15) and equations resulting from the derivatives of (4.4) and (4.10) with respect to time parameter $\bar{\rho}_0$, and obtain a Volterra integral equation of the second kind, i.e.

$$\dot{\bar{\sigma}}(R, \bar{\rho}_0) = F_1(R, \bar{\rho}_0) + \int_R^{\bar{\rho}_0} K(R, y, \bar{\rho}_0)\dot{\bar{\sigma}}(y, \bar{\rho}_0)\,dy, \tag{4.16}$$

where the value of $\bar{\rho}_0$ is fixed and F_1 and K are given for a given state as functions of R, $\bar{\sigma}$, m and $\bar{\rho}_0$. The usual method of successive approximation [13] can now be applied to (4.16) to obtain the rate $\dot{\bar{\sigma}}(R, \bar{\rho}_0)$ in the region $1 \leq R \leq \bar{\rho}_0$ for a given state.

For the special loading program

$$m = m_0 = \text{constant}, \tag{4.17}$$

the basic unknown $\bar{\sigma}(R, \bar{\rho}_0)$ can be obtained in a simple way. Indeed, for the loading

program (4.17) and subject to the conditions $\varepsilon_\theta'' = 0$ and $\bar{\sigma} = 1$ at $R = \bar{\rho}_0$, and ε_θ'' for $R < \bar{\rho}_0$ given by (4.10), we can integrate (4.11) with respect to the time parameter $\bar{\rho}_0$ to obtain

$$\begin{aligned} G_1(\bar{\sigma}, R, \bar{\rho}_0) &\equiv \mathscr{H}(\bar{\sigma}, R, \bar{\rho}_0) - \frac{n\eta(1-\nu)}{(\beta-n)(2-n)}\left[\left(\frac{\bar{\rho}_0}{R}\right)^2 - \left(\frac{\bar{\rho}_0}{R}\right)^n\right]\psi(1, \bar{\rho}_0) \\ &= \frac{n\eta(1-\nu)}{2-n}\int_R^{\bar{\rho}_0} (R^{-2}y - R^n y^{n-1})\psi(\bar{\sigma}, y)\,\mathrm{d}y, \quad \text{for } n \neq 2, \end{aligned} \tag{4.18a}$$

and

$$\begin{aligned} G_2(\bar{\sigma}, R, \bar{\rho}_0) &\equiv \mathscr{H}(\bar{\sigma}, R, \bar{\rho}_0) - \frac{2\eta(1-\nu)}{\beta-n}\left(\frac{\bar{\rho}_0}{R}\right)^2 \ln\left(\frac{\bar{\rho}_0}{R}\right)\psi(1, \bar{\rho}_0) \\ &= 2\eta(1-\nu)R^{-2}\int_R^{\bar{\rho}_0} y(\ln y - \ln R)\psi(\bar{\sigma}, y)\,\mathrm{d}y, \quad \text{for } n = 2, \end{aligned} \tag{4.18b}$$

where

$$\mathscr{H}(\bar{\sigma}, R, \bar{\rho}_0) = \ln\{[\bar{\sigma} + \psi(\bar{\sigma}, R)]/[1 + \psi(1, R)]\} + \psi(1, R) - (\bar{\sigma}^{-1} - \eta)\psi(\bar{\sigma}, R) - \eta\left(\frac{\bar{\rho}_0}{R}\right)^2 \psi(1, \bar{\rho}_0), \tag{4.18c}$$

and

$$\eta \equiv \frac{a\sigma_0}{E} \equiv \frac{a}{\bar{E}}. \tag{4.18d}$$

Equation (4.18a) or (4.18b) is to be solved for $\bar{\sigma}(R, \bar{\rho}_0)$, where $1 \leq R \leq \bar{\rho}_0$, and $\bar{\rho}_0$ is fixed. Since for metals the ratio σ_0/E is of the order of 10^{-3}, η defined in (4.18d) is a small quantity for the usual values of the work-hardening parameter, a. It is noted that for $\eta = 0$ (non-hardening materials), (4.18a, b) have the solution $\bar{\sigma}(R, \bar{\rho}_0) = 1$. For the very special case of a uniform disk, $n = 0$, the integral on the right-hand side of equation (4.18a) vanishes, and the solution $\bar{\sigma}(R, \bar{\rho}_0)$ then corresponds to the zeros of the algebraic function $G_1(\bar{\sigma}, R, \bar{\rho}_0) = 0$. For $\eta \neq 0$ and $n \neq 0$, the solution $\bar{\sigma}_r(R, \bar{\rho}_0)$ at a fixed $\bar{\rho}_0$, can be obtained either by a successive approximation or by a perturbation method with η as the perturbation parameter.

To use the method of successive approximation, we may begin with an initial approximation $\bar{\sigma}^{(0)}(R, \bar{\rho}_0)$, which is obtained by setting G_1 equal to zero†, and evaluate the right-hand side of (4.18a), resulting in, say, $C(R, \bar{\rho}_0)$. The next approximation can then be obtained by setting $G_1 - C$ equal to zero; in order to have a better approximation the more accurate values of $\bar{\sigma}$ may be used to evaluate C as soon as they are available. We repeat this procedure until it converges to an accurate result. For intermediate values of the load parameters, for which (4.13) is satisfied, and for usual value of a, say $a \sim 10$, the right-hand sides of equations (4.18a, b) are small quantities. Hence, the successive approximation is rapidly convergent. For instance, with $n = 1$, $\nu = 0{\cdot}3$, $\sigma_0/E = 10^{-3}$, $a = 10$ and at $m_0 = 0{\cdot}9$ and $\bar{\rho}_0 = 1{\cdot}1$ (which corresponds to $P = 0{\cdot}6117$), the results of the first and second iterations agree with each other up to eight figures.

For small values of η, we may use a perturbation technique by setting

$$\bar{\sigma}(R, \bar{\rho}_0) = 1 + \eta\Phi_1(R, \bar{\rho}_0) + \eta^2\Phi_2(R, \bar{\rho}_0) + \ldots. \tag{4.19}$$

† For $n = 2$, G_1 must be replaced by G_2, equation (4.18b).

As a first-order perturbation solution to (4.18a, b), we find

$$\Phi_1(R,\bar{\rho}_0) = -1+\frac{\psi(1,\bar{\rho}_0)}{\psi(1,R)}\left\{\left(\frac{\bar{\rho}_0}{R}\right)^2+\frac{n(1-\nu)}{(\beta-n)(2-n)}\left[\left(\frac{\bar{\rho}_0}{R}\right)^2-\left(\frac{\bar{\rho}_0}{R}\right)^n\right]\right\}$$
$$+\frac{n(1-\nu)}{2-n}\frac{1}{\psi(1,r)}\int_R^{\bar{\rho}_0}(R^{-2}y-R^{-n}y^{n-1})\psi(1,y)\,dy, \quad \text{for } n\neq 2, \tag{4.20a}$$

and

$$\Phi_1(R,\bar{\rho}_0) = -1+\frac{\psi(1,\bar{\rho}_0)}{\psi(1,R)}\left(\frac{\bar{\rho}_0}{R}\right)^2\left[1+\frac{2(1-\nu)}{\beta-n}\ln\left(\frac{\bar{\rho}_0}{R}\right)\right]$$
$$+\frac{2(1-\nu)}{\psi(1,R)}R^{-2}\int_R^{\bar{\rho}_0}y(\ln y-\ln R)\psi(1,y)\,dy \quad \text{for } n=2. \tag{4.20b}$$

We observe that since (4.20a, b) give $\Phi_1(\bar{\rho}_0,\bar{\rho}_0)=0$, the two-term approximation of (2.24) yields $\bar{\sigma}(\bar{\rho}_0,\bar{\rho}_0)=1$ as should be expected. While the perturbation solution gives an exact value for $\bar{\sigma}$ at $R=\bar{\rho}_0$, the result it predicts becomes less accurate when R is close to 1. An extreme example is given by the case when $m_0=1$ for which $\bar{\rho}(R,\bar{\rho}_0)$ approaches to infinity as R approaches to 1. For $m_0<1$, say $m_0=0.9$, and small η, the two-term perturbation solution given by (4.20) and (4.19) yields fairly accurate results.

As a numerical example, we consider the case when $n=1$, $\sigma_0/E=10^{-3}$, $\nu=0{\cdot}3$, $m_0=0{\cdot}9$ and $\bar{\rho}_0=1{\cdot}1$. The distributions of yield stress $\bar{\sigma}(R,\bar{\rho}_0)$ obtained by a two-term perturbation solution and by a successive approximation† are compared in Fig. 7 for

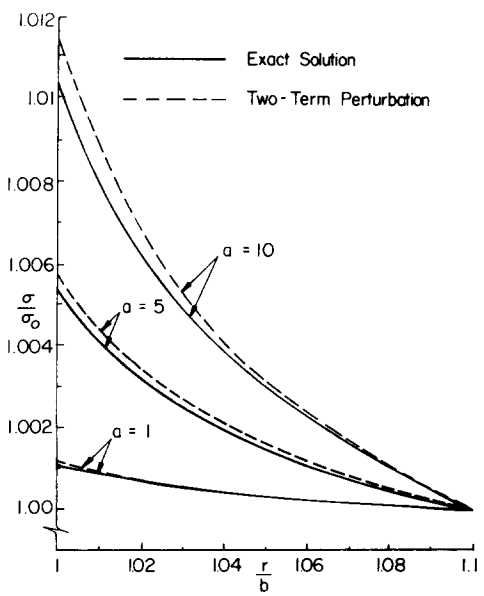

FIG. 7. Comparison between two-term perturbations and exact solutions of equation (4.18); $n=1$, $\sigma_0/E=10^{-3}$, $\nu=0{\cdot}3$, $m_0=0{\cdot}9$, $\bar{\rho}_0=1{\cdot}1$ and indicated values of a.

† Since the results obtained by the successive approximation can be made as accurate as we please, the corresponding solution may be viewed as "exact".

the indicated values of a; note that $\eta = 10^{-2}$ for $a = 10$. As is evident from Fig. 7, for $a = 1$, the results predicted by these two methods agree very well with each other, and for $a = 10$ the discrepancy becomes larger only for points at the vicinity of the hole. For a more accurate comparison, Table 2 displays the yield stress $\bar{\sigma}$ at the edge of the hole and the value of P which is calculated according to (4.4) when $\bar{\sigma}$ is determined for $1 \leq R \leq \bar{\rho}_0$. It is interesting to note that, for given m_0 and $\bar{\rho}_0$, and for large values of a, say, $a = 10$, the value of the yield stress at the edge of the hole, obtained by the two-term perturbation solution, is in error by 0·11 per cent, while the error in the value of P is only 0·01 per cent.

TABLE 2. COMPARISON BETWEEN TWO-TERM PERTURBATION AND EXACT SOLUTIONS OF (4.18); $n = 1$, $\sigma_0/E = 10^{-3}$, $\nu = 0{\cdot}3$, $m_0 = 0{\cdot}9$, $\bar{\rho}_0 = 1{\cdot}1$ AND a AS INDICATED P IS CALCULATED ACCORDING TO EQUATION (4.4)

a	1		2		3	
	Two-term perturbation	Exact	Two-term perturbation	Exact	Two-term perturbation	Exact
P	0·611162	0·611159	0·611234	0·611227	0·611306	0·611294
$\sigma(b)/\sigma_0$	1·001139	1·001087	1·002277	1·002159	1·003416	1·003217
a	4		5		10	
	Two-term perturbation	Exact	Two-term perturbation	Exact	Two-term perturbation	Exact
P	0·611377	0·611361	0·611449	0·611427	0·611804	0·611747
$\sigma(b)/\sigma_0$	1·004555	1·004260	1·005694	1·005291	1·011387	1·010253

B. *Discussion and numerical results*

For the values of the load parameters m and P such that neither (4.13) nor (3.8) is violated, the distributions of the shearing stress $\bar{\sigma}_{r\theta}$ for elastic–plastic and rigid–plastic disks are exactly the same, as given by (2.18). The stress components $\bar{\sigma}_r$ and $\bar{\sigma}_\theta$ in the elastic region, $R > \bar{\rho}_0$, of an elastic–plastic disk differ from those in the rigid region, $R > \rho_0$, of a rigid–plastic disk only because of the Poisson ratio ν, where $\bar{\rho}_0$ denotes the radius of the elastic–plastic, and ρ_0 that of the rigid–plastic interface; $\nu = \frac{1}{2}$ for rigid–plastic and $0 \leq \nu \leq \frac{1}{2}$ for elastic–plastic materials. However, the presence of the elastic strains and hardening effect will render the stress components $\bar{\sigma}_r$ and $\bar{\sigma}_\theta$ in the elastic–plastic region, $1 \leq R \leq \bar{\rho}_0$, of an elastic–plastic disk different from those in the neutral plastic region, $1 \leq R \leq \rho_0$, of the corresponding rigid–plastic disk.

To illustrate the effect of elastic strains and hardening on the solution, we consider an example of a conical ($n = 1$) elastic–plastic disk with $\sigma_0/E = 10^{-3}$, $\nu = 0{\cdot}3$, arbitrary a, and under the loads $m_0 = 0{\cdot}9$ and $P = 0{\cdot}611747$ attained by the loading program (4.17). It is found that the dimensionless radial displacement U_r at the edge of the hole equals to $0{\cdot}5050 \times 10^{-3}$ for $a = 1$, and to $0{\cdot}5040 \times 10^{-3}$ for $a = 10$; since this displacement is of the order of the elastic displacement and is affected only slightly by the hardening parameter a, the result obtained assuming a rigid–plastic material appears to be a good approximation. The distributions of stress components $\bar{\sigma}_r$ and $\bar{\sigma}_\theta$ for $a = 1$, 5 and 10, are given in Table 3 where the corresponding results for the rigid–plastic disk are also reported for comparison. As can be seen from Table 3, for an elastic–plastic disk, the effect of the hardening parameter,

TABLE 3. COMPARISON OF STRESSES FOR ELASTIC–PLASTIC AND RIGID–PLASTIC SOLUTIONS; $n = 1$, $\sigma_0/E = 10^{-3}$, $\nu = 0{\cdot}3$, $m_0 = 0{\cdot}9$, $P = 0{\cdot}611747$ AND a AS INDICATED

r/b		1		1·02		1·04	
	a	$-\sigma_r/\sigma_0$	σ_θ/σ_0	$-\sigma_r/\sigma_0$	σ_θ/σ_0	$-\sigma_r/\sigma_0$	σ_θ/σ_0
Elastic–plastic	1	0·611747	−0·173365	0·586000	−0·054927	0·562069	0·038459
	5	0·611747	−0·163841	0·585992	−0·050165	0·562055	0·041047
	10	0·611747	−0·152824	0·585982	−0·044467	0·562035	0·044182
Rigid–plastic		0·611747	−0·175857	0·590233	−0·060381	0·567991	0·031880
r/b		1·06		1·08		1·10	
	a	$-\sigma_r/\sigma_0$	σ_θ/σ_0	$-\sigma_r/\sigma_0$	σ_θ/σ_0	$-\sigma_r/\sigma_0$	σ_θ/σ_0
Elastic–plastic	1	0·539963	0·115345	0·519457	0·180371	0·500372	0·236362
	5	0·539942	0·116706	0·519431	0·180950	0·500344	0·236393
	10	0·539914	0·118365	0·519397	0·181650	0·500308	0·236425
Rigid–plastic		0·545417	0·109551	0·522760	0·176928	0·500576	0·183223

a, on the stress component $\bar{\sigma}_r$ is negligible, while the stress component $\bar{\sigma}_\theta$ is only slightly affected by a. The distribution of stress component $\bar{\sigma}_\theta$ for an elastic–plastic disk is considerably different from that for a rigid–plastic disk only when a is large; this can be expected because the solution in the neutral plastic region of a rigid–plastic material is independent of a. However, the difference between the distributions of the stress component $\bar{\sigma}_r$ for an elastic–plastic and a rigid–plastic disk is small; this is not strange because both disks must satisfy the same boundary condition $\bar{\sigma}_r(R) = -P$ at $R = 1$.

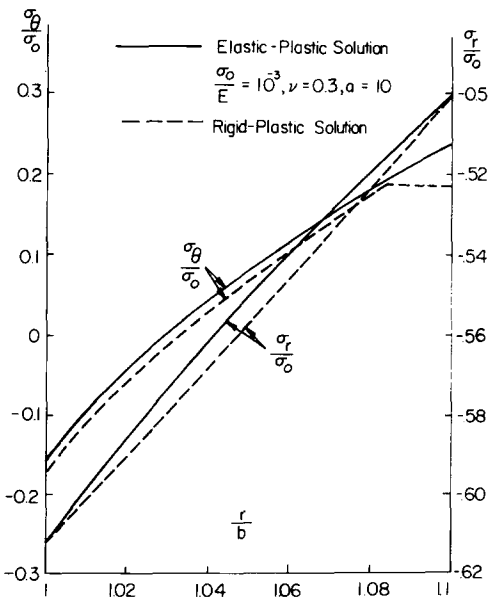

FIG. 8. Comparison of stresses for elastic–plastic and rigid–plastic solutions; $n = 1$, $m_0 = 0{\cdot}9$ and $P = 0{\cdot}611747$.

Figure 8 compares stresses obtained for elastic–plastic and rigid–plastic solutions, where the value of a for the elastic–plastic disk is taken to be 10. It is noted that under the loadings considered here, $\bar{\rho}_0 = 1{\cdot}1$ and $\rho_0 = 1{\cdot}084$; the discontinuity of the slope of $\bar{\sigma}_\theta$ at $R = \bar{\rho}_0$ for the elastic–plastic disk, and that at $R = \rho_0$ for the rigid–plastic disk, make the distribution of $\bar{\sigma}_\theta$ for each of these two disks considerably different from the other in the region $\rho_0 \leq R \leq \bar{\rho}_0$ and immediately outside of $\bar{\rho}_0$. On the other hand, the distributions of the corresponding radial stress $\bar{\sigma}_r$ in these regions do not differ from each other significantly, see Fig. 8.

REFERENCES

[1] G. I. TAYLOR, The formation and enlargement of a circular hole in a thin plastic sheet. *Q. J. Mech. appl. Math.* **1**, 103–124 (1948).
[2] R. HILL, Plastic distortion of nonuniform sheets. *Phil. Mag.* **40**, 971–983 (1949).
[3] W. PRAGER, On the use of singular yield conditions and associated flow rules. *J. appl. Mech.* **20**, 317–320 (1953).
[4] P. G. HODGE, JR. and R. SANKARANARAYANAN, On finite expansion of a hole in a thin infinite plate. *Q. appl. Math.* **16**, 73–80 (1958).
[5] J. N. ALEXANDER and H. FORD, On expanding a hole from zero radius in a thin infinite plate. *Proc. R. Soc.* **A226**, 543–561 (1954).
[6] T. G. ROGERS, The finite expansion and subsequent unloading of a hole in an elastic–plastic plate of initially varying thickness. *Q. J. Mech. appl. Math.* **20**, 137–166 (1967).
[7] S. NEMAT-NASSER, Finite expansion of a hole in a rigid–workhardening disk of initially non-uniform thickness. *J. Mech. Phys. Solids* **16**, 196–204 (1968).
[8] J. N. CHERN and S. NEMAT-NASSER, The enlargement of a hole in a rigid–workhardening disk of non-uniform initial thickness. *J. Mech. Phys. Solids* **17**, 271–289 (1969).
[9] J. M. CHERN, Expansion of a hole in a disk with kinematic hardening. *Int. J. Mech. Sci.* **11**, 623–632 (1969).
[10] R. P. NORDGREN and P. M. NAGHDI, Finite twisting and expansion of a hole in a rigid/plastic plate. *J. appl. Mech.* **30**, 605–612 (1963).
[11] R. P. NORDGREN and P. M. NAGHDI, Loading and unloading solutions for an elastic/plastic annular plate in the state of plane stress under combined pressure and couple, *Int. J. Engng Sci.* **1**, 33–70 (1963).
[12] A. RALSTON and H. WILF, *Mathematical Methods for Digital Computers*, pp. 110–120. Wiley (1960).
[13] R. A. BUCKLINGHAM, *Numerical Methods*, p. 346. Pitman (1957).

(*Received* 7 *July* 1969)

Абстракт—Обсуждается конечная и инфинитезимальная деформация бесконечно распространяющегося осесимметрического диска, неравномерной начальной толщины, с круглым отверстием. Диск нагружен давлением и крутящим моментом неуменьшающейся величины, вдоль внутренней поверхности отверстия. Предполагается плоское напряженное состояние, при использовании теории пластического течения. Принимается, что материал диска жестко-пластический для конечных деформаций и упруго-пластический для инфинитезимальных деформаций. Анализ основан на критерии текучести Трески и законе изотропного упрочнения. Обращается особое внимание на эффекты крутящего момента, параметре упрочнения и траектории нагрузки в решению. Даются подробные результаты и сравнения для начально равномерного и начально конического диска. Наконец, приводится сравнение между решениями для упруго-пласти-ческих и жестко-пластических дисков. Оно показывает, что поле напряжений находится только слегка под влиянием упругих деформаций.